Joint User Selection and Beamforming Design for Multi-IRS Aided Internet-of-Things Networks

Seok-Hyun Yoon, *Student Member, IEEE*, Byungju Lim, *Member, IEEE*, Mai Vu, *Senior Member, IEEE*, and Young-Chai Ko, *Senior Member, IEEE*

***Abstract*—Intelligent reflecting surface (IRS) has recently emerged as a promising technology for Internet-of-Things (IoT) networks to provide massive connectivity. In this article, we propose IoT user selection methods and beamforming designs in a multi-IRS aided IoT network. Specifically, we aim to jointly optimize the base station (BS) beamforming, IRS reflection coefficients and user selection to maximize the weighted sum rate of selected users, which is a mixed integer non-linear (MINLP) problem. To solve this MINLP problem, we design a novel algorithm by absorbing user selection implicitly into BS beamforming design, and applying a fractional programming (FP) to alternate between BS beamforming design using a Lagrangian-based subgradient method and IRS coefficients optimization using a complex circle manifold (CCM) method. However, this algorithm has high complexity, thus we further propose two low complexity and non-alternating algorithms, one using a channel correlation based metric for user selection, and the other using zero-forcing (ZF) beamforming at the BS. Numerical results show that our proposed algorithms achieve significant performance gain over benchmark schemes, and the low complexity algorithms achieve a performance comparable with the joint optimization algorithm at a fraction of the run time. These algorithms demonstrate that multiple IRSs help improve the network sum rate, IRSs with more elements tend to select IoT users more close by, and the best locations for IRS placement are near IoT device clusters.**

***Index Terms*—Intelligent reflecting surface (IRS), multi-IRS, IoT, user selection, beamforming, weighted l_1-norm approximation, and 6G networks.**

I. Introduction

With the ever-increasing demand of mobile traffic and the number of connected devices in 5G and beyond Internet-of-Things (IoT) networks, the future 6G IoT networks will support much higher number of devices while achieving ultra-high data rate and energy efficiency [1]. To achieve these requirements in 5G and beyond IoT networks, key technologies including mmWave and sub-THz communications, massive MIMO, and ultra dense network (UDN) provide potential solutions, but require high hardware cost and large energy consumption because of the need to employ many base stations (BSs) within a certain area and a large number of antennas at each BS. New technologies are needed to achieve sustainable high performance at an affordable cost in 6G IoT networks.

Recently, intelligent reflecting surface (IRS) technology has shown promises regarding the above issues [2]. An IRS employs a 2D planar surface composed of a large number of passive elements supported by recently advanced micro electromechanical systems (MEMS) and metamaterials. Each element can individually control the reflected phase and amplitude of an incident wave, which can then be used to alter the reflection channel environment. Since an IRS simply reflects the signal using passive elements without RF chains or digital signal processor (DSP), its hardware costs and energy consumption can be kept to a minimal level. By adjusting the amplitude and phase of each element, the reflected signal from an IRS can be coherently combined with the direct signal from BS and helps enhance the data rate. Also, since an IRS is able to create a virtual line-of-sight (LoS) link for bypassing obstacles, it can enhance the cell coverage. In addition, multiple IRSs can be easily installed on the wall and ceiling of a building and integrated with the existing cellular system. Thanks to these advantages, IRS is being considered as a key technology for achieving high data rate with low cost and low energy consumption in the 6G IoT network.

A. Related Works

Most of existing works assume networks aided by a single IRS [3], [4], [5], [6], [7], [8], [9], [10], [11], [12], but in practical systems, there are many advantages of deploying multiple IRSs. First, by deploying multiple IRSs, it is easier to create a virtual line-of-sight (LoS) link between the IRSs and a user since the distance between an IRS and the user can be reduced. Moreover, we can exploit multiple reflected signals from multiple IRSs and combine them at the receiver to significantly enhance the received signal power while mitigating the interference to other users. Several works in the literature have considered a multi-IRS aided single cell system [13], [14], [15], [16], [17]. An optimization framework to maximize the weighted sum rate of all cell-edge users aided by multiple IRSs is proposed in [13]. In [14], the BS beamforming and each IRS's phase

Manuscript received 31 March 2023; revised 25 July 2023 and 29 August 2023; accepted 2 September 2023. Date of publication 11 September 2023; date of current version 13 February 2024. This work was supported by the MSIT (Ministry of Science and ICT), Korea, under the ITRC (Information Technology Research Center) support program under Grant IITP-2023-2021-0-01810 supervised by the IITP (Institute for Information & Communications Technology Planning & Evaluation). The review of this article was coordinated by Dr. Chau Yuen. *(Corresponding authors: Byungju Lim; Young-Chai Ko.)*

Seok-Hyun Yoon and Young-Chai Ko are with the School of Electrical Engineering, Korea University, Seoul 02841, South Korea (e-mail: daniel419@korea.ac.kr; koyc@korea.ac.kr).

Byungju Lim is with the Department of Electrical Engineering, Pukyong National University, Busan 48513, South Korea (e-mail: limbj@pknu.ac.kr).

Mai Vu is with the Department of Electrical and Computer Engineering, Tufts University, Medford, MA 02155 USA (e-mail: mai.vu@tufts.edu).

Digital Object Identifier 10.1109/TVT.2023.3313606

0018-9545 © 2023 IEEE. Personal use is permitted, but republication/redistribution requires IEEE permission.
See https://www.ieee.org/publications/rights/index.html for more information.

Authorized licensed use limited to: Univ Of Incheon. Downloaded on October 26,2026 at 13:11:01 UTC from IEEE Xplore. Restrictions apply.

shifts in a multi-IRS aided mmWave system are optimized to produce a near-optimal analytical solution. This result shows that more IRSs deployed in a network leads to more virtual LoS links making it robust against blockages especially in mmWave communications. In [15], a multi-IRS setting is exploited to enhance the weighted sum rate in full-duplex systems under hardware impairments. Both the transmit and receive beamforming vectors at BS, the transmit powers of the uplink users, and the phase shifts of each IRS are jointly optimized by using an efficient iterative alternating approach. For maximizing the energy efficiency of a system, the authors in [16] jointly optimize the reflection coefficients and on-off status of IRSs. They show that a multi-IRS system achieves higher energy efficiency than amplify-and-forward (AF) relaying because of the low power consumption at IRSs. In [17], IRS-user association is considered to reduce the channel estimation complexity in a multi-IRS aided single cell system.

In most of existing works, the BS supports all users located in a cell and designs the operating parameters for those users. However, when a massive number of users are deployed such as in IoT networks, it is not feasible to support more users than the number of BS antennas in the same time-frequency resource block. Accordingly, the BS should appropriately select a number of users up to the number of BS antennas to maximize the system performance. Although many researchers have conducted the joint design of BS beamforming and user selection in a cellular network without IRS [18], [19], [20], [21], it is impossible to apply these algorithms in an IRS-aided network, since the channels can be reconfigured by controlling the amplitude and phase of IRS elements for selected users. This difficulty leads to the need for a new user selection method with the consideration of IRS phase shifts control in an IRS-aided system.

However, it is challenging to jointly optimize the BS beamforming, IRS phase shifts and user selection since they are coupled in the optimization problem. To solve the problem, most of existing works have adopted machine learning approaches [22], [23]. In [22], neural combinatorial optimization (NCO) technique and deep deterministic policy gradient (DDPG) are used to jointly design the above variables to maximize the weighted sum rate in an IRS-aided single cell uplink system. In [23], optimizing the user selection, time resource allocation and IRS's phase shifts in IRS-aided vehicular communication system is considered using a deep reinforcement learning (DRL) based optimization framework. All these works only considered single-IRS assisted wireless networks, thus the DL/RL structure must be modified and retrained to incorporate multiple IRSs, since input and output sizes of the employed neural networks are dependent on the size of optimization variables. In other words, the trained neural networks cannot be applicable to other network settings such as a multiple IRSs aided network due to the fixed input and output dimensions in fully connected layers [24].

B. Our Contributions

In this article, we propose several scalable, customized and efficient user selection and beamforming algorithms for a multi-IRS aided IoT network. Different from the few existing works on this topic which rely on machine learning as discussed above, our work uses traditional optimization methods to jointly perform user selection and beamforming design. Our main contributions are summarized as follows.

- The joint optimization of BS beamforming, IRS reflection coefficients and user selection to maximize the weighted sum rate is an NP-hard optimization problem which has not been studied in literature. We design a novel iterative algorithm which alternatively optimizes the BS beamforming and IRS reflection coefficients, while incorporating user selection implicitly into the BS beamforming which reduces the number of optimization variables, and thus can introduce a lower complexity.
- Specifically, we incorporate the user selection constraint into a non-smooth l_0-norm constraint for the BS beamforming and approximate it with a smooth, weighted l_1-norm constraint. The l_1-norm approximation for user selection make the optimization a new and challenging problem, which to the best our knowledge, has not been addressed in the literature. We then use a fractional programming (FP) based block coordinate descent (BCD) method to divide the problem into two tractable subproblems. To optimize the BS beamforming with implicit user selection, we transform the subproblem into a convex form using a quadratic transform FP method and solve it with a Lagrangian-based subgradient method. For optimizing the IRS reflection coefficients, we adopt both a quadratic transform FP method and a complex circle manifold (CCM) method to overcome the non-convex unit modulus constraint of IRS phase shifts.
- In addition, we propose two low-complexity, non-alternating user selection algorithms. The first algorithm uses a novel channel correlation metric to select users, and then jointly optimizes the BS beamforming and the IRS reflection coefficients using the above FP-based BCD algorithms. The second algorithm selects users in a greedy manner based on the observation that each IRS may have the most significant impact on the users closest to it. In particular, it employs ZF beamforming with water-filling power allocation and controls the IRS coefficients to align the phase of the direct link with that of the reflected link for the nearest user during each iteration.
- Numerical results show that the proposed algorithms achieve a better sum rate performance compared to benchmark algorithms, and there exists a trade-off between complexity and the performance among proposed algorithms. Furthermore, the proposed algorithms allow us to analyze in detail the effects of key system parameters, including the number of IRS elements, IRSs, users and IRS location. Our analysis shows the sum rate enhancement benefit of using multiple IRSs and selecting user clusters near each IRS, and also provides a guidance to the optimal locations for IRS placements in the network.

The rest of this article is organized as follows. In Section II, we present the system model. In Section III, we formulate the joint BS beamforming, IRS reflection coefficients, and IoT user selection optimization problem and reformulate this problem based on weighted l_1-norm approximation and FP-based BCD

Authorized licensed use limited to: Univ Of Incheon. Downloaded on October 26,2026 at 13:11:01 UTC from IEEE Xplore. Restrictions apply.

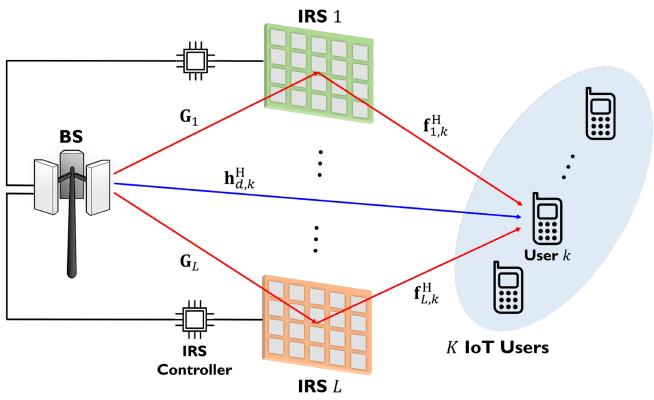


Fig. 1. Multi-IRS aided IoT networks.

method. In Section IV, we present the Lagrangian-based subgradient method for joint BS beanforming design and user selection, and in Section V, we present the Complex Circle method for IRS reflection coefficients design. In Section VI, we summarize the overall algorithm and analyze its computational complexity. Then, in Section VII, we present the two low complexity heuristic algorithms. In Section VIII, we present numerical results to evaluate the performance of the proposed algorithms. In Section IX, we draw our conclusions.

Notation: a, $\mathbf{a}$ and $\mathbf{A}$ is a scalar, a column vector and a matrix, respectively. The conjugate, transpose, Hermitian, and matrix inversion are denoted as $(\cdot)^*$, $(\cdot)^{\mathsf{T}}$, $(\cdot)^{\mathsf{H}}$, and $(\cdot)^{-1}$, respectively. $\mathbb{C}^{N\times M}$ and $\mathbb{R}^{N\times M}$ denotes the space of $N\times M$ complex and real matrix, respectively. $\mathbf{I}_M$ and $\mathbf{0}_M$ is an identity matrix and a zero matrix of size $M\times M$, respectively. $[\mathbf{A}]_{n,m}$ denotes the element at the n-th row and the m-th column of matrix $\mathbf{A}$. For a complex scalar a, its conjugate, amplitude and phase are denoted as a^*, $|a|$ and $\angle(a)$, respectively. For a vector $\mathbf{a}$, $\|\mathbf{a}\|$ and $|\mathbf{a}|_p$ denotes l_2-norm and l_p-norm, respectively, and $\mathbf{A}=\mathsf{diag}(\mathbf{a})$ is a diagonal matrix with the elements of $\mathbf{a}$ on its diagonal. $|\mathcal{A}|$ denotes the cardinality of set $\mathcal{A}$. $\binom{n}{k}$ denotes the number of k combinations of n elements, $\odot$ denotes the Hadamard product, $\mathrm{Re}\{\cdot\}$ denotes the real part of its argument, $\mathcal{O}(\cdot)$ denotes big-O for describing the order of complexity and function $[x]_+$ denotes $\max[0,x]$.

II. System Model

A. Network Model

We consider a multi-IRS aided multi-user downlink system, where L distributed IRSs are deployed to assist communications from a BS to a set of K single antenna IoT users, as shown in Fig. 1. The BS is equipped with M antenna arrays where a uniform linear array (ULA) structure is implemented and each IRS is equipped with $N=N_hN_v$ antenna arrays configured in a form of uniform planar array (UPA) where N_h and N_v are the numbers of antenna elements in horizontal and vertical direction, respectively. We assume a crowded hotspot scenario, so there exists many cell-edge users which is much larger than the number of BS antennas, i.e., $K >> M$. Note that the passive elements in each IRS are controlled by an IRS controller that communicates with BS over a separate backhaul link. Let the sets of IRSs, users, and the reflecting elements of each IRS denote as $\mathcal{L}\triangleq\{1,2,\ldots,L\}$, $\mathcal{K}\triangleq\{1,2,\ldots,K\}$, and $\mathcal{N}\triangleq\{1,2,\ldots,N\}$. In addition, $\mathbf{\Theta}_l=\mathsf{diag}(\theta_{l,1},\ldots,\theta_{l,N})$ is defined as a diagonal reflection coefficients matrix of the l-th IRS with $\theta_{l,n}=e^{j\phi_{l,n}}$, where $\phi_{l,n}\in[0,2\pi)$ represents a phase shift of its n-th reflecting element. For IRS phase shifts design, we assume continuous phase shift and unit reflection amplitude for each element.

B. Channel Model

We adopt a quasi-static block fading channel model where all the channels are assumed to be constant in each coherence block. Let $\mathbf{G}_l\in\mathbb{C}^{N\times M}$, and $\mathbf{f}_{l,k}\in\mathbb{C}^{N\times 1}$ denote a channel between BS and the l-th IRS, and a channel between the l-th IRS and the k-th user, respectively. For a practical IRS-aided environment, both LoS and NLoS paths exist in the BS-IRS and IRS-user channel. Then, $\mathbf{G}_l$ and $\mathbf{f}_{l,k}$ can be modeled as Rician fading channel given by

$$\mathbf{G}_l=\sqrt{\alpha_l}\left(\sqrt{\frac{\kappa_{\mathsf{BI}}}{\kappa_{\mathsf{BI}}+1}}\bar{\mathbf{G}}_l+\sqrt{\frac{1}{\kappa_{\mathsf{BI}}+1}}\hat{\mathbf{G}}_l\right), \tag{1}$$

$$\mathbf{f}_{l,k}=\sqrt{\alpha_{l,k}}\left(\sqrt{\frac{\kappa_{\mathsf{IU}}}{\kappa_{\mathsf{IU}}+1}}\bar{\mathbf{f}}_{l,k}+\sqrt{\frac{1}{\kappa_{\mathsf{IU}}+1}}\hat{\mathbf{f}}_{l,k}\right), \tag{2}$$

where α_l and $\alpha_{l,k}$ are the large-scale fading coefficients of $\mathbf{G}_l$ and $\mathbf{f}_{l,k}$, respectively, and κ_{BI} and κ_{IU} are Rician K factors of the BS-IRS channel and the IRS-user channel, respectively. Also, $\bar{\mathbf{G}}_l$ and $\bar{\mathbf{f}}_{l,k}$ denote the components of deterministic LoS channels and $\hat{\mathbf{G}}_l$ and $\hat{\mathbf{f}}_{l,k}$ are the NLoS channel components whose entries are independent and identically distributed (i.i.d.) complex Gaussian random variables with zero mean and unit variance.

To characterize the LoS channel, we first define a $J\times 1$ array response vector of ULA and UPA with $J_h\times J_v$ as

$$\mathbf{a}_{\mathrm{ULA}}(\vartheta^a,J)=\mathbf{u}(\sin\vartheta^a,J), \tag{3}$$

$$\mathbf{a}_{\mathrm{UPA}}(\vartheta^a,\vartheta^e,J)=\mathbf{u}(\sin\vartheta^a\cos\vartheta^e,J_h)\otimes\mathbf{u}(\sin\vartheta^e,J_v), \tag{4}$$

where ϑ^a and ϑ^e are the azimuth and the elevation angles of departure (AoD) or the angle of arrival (AoA), and $\mathbf{u}(\vartheta^a,J)\triangleq[1,e^{j2\pi\frac{d}{\lambda}\vartheta^a},\cdots,e^{j2\pi(J-1)\frac{d}{\lambda}\vartheta^a}]^{\mathrm{T}}$. From (3) and (4), $\bar{\mathbf{G}}_l$ and $\bar{\mathbf{f}}_{l,k}$ can be expressed as

$$\bar{\mathbf{G}}_l=\mathbf{a}_{\mathrm{UPA}}(\vartheta_l^a,\vartheta_l{}^e,N)\,\mathbf{a}_{\mathrm{ULA}}(\varphi_l^a,M)^{\mathrm{H}}, \tag{5}$$

$$\bar{\mathbf{f}}_{l,k}=\mathbf{a}_{\mathrm{UPA}}(\vartheta_{l,k}^a,\vartheta_{l,k}^e,N)^{\mathrm{H}}, \tag{6}$$

where φ_l^a and $\vartheta_l^a/\vartheta_l^e$ are LoS AoD and elevation/azimuth AoA between BS and the l-th IRS, and $\vartheta_{l,k}^a/\vartheta_{l,k}^e$ are LoS elevation/azimuth AoD between the l-th IRS and the k-th user.

Furthermore, the direct channel between BS and the k-th user, $\mathbf{h}_{d,k}\in\mathbb{C}^{M\times 1}$, is assumed to be Rayleigh fading which is given by

$$\mathbf{h}_{d,k}=\sqrt{\alpha_{d,k}}\,\hat{\mathbf{h}}_{d,k}. \tag{7}$$

Authorized licensed use limited to: Univ Of Incheon. Downloaded on October 26,2026 at 13:11:01 UTC from IEEE Xplore. Restrictions apply.

where $\alpha_{d,k}$ is a large-scale fading coefficient and the entries of $\hat{\mathbf{h}}_{d,k}$ are i.i.d. complex Gaussian random variables with zero mean and unit variance. We assume that BS obtains perfect channel state information (CSI) of the direct link and the reflected links as commonly assumed in the literature [3]. CSI can be obtained by utilizing various channel estimation schemes specifically designed for an IRS-aided network, such as an efficient parallel factor decomposition method [9], or a three-phase pilot based channel estimation framework [10]. By assuming perfect CSI, the performance of our algorithms will provide an upper bound for the sum rate achievable in practice. However, all the analysis and conclusion on the impact of multiple IRSs, IRS sizes and their placement will also hold for other types of CSI and therefore provide practical insights.

C. Signal Model

For achieving spatial multiplexing gain, BS cannot support more users than the number of antennas in the same time-frequency resource block. Therefore, BS needs to select at most M users which maximize the network utility function. To represent this, we define a binary selection indicator $\mathbf{a} = [a_1, \ldots, a_K]^{\mathsf{T}}$ which satisfies

$$a_k = \begin{cases} 1, & \text{if} k\text{-th user is selected,} \\ 0, & \text{otherwise.} \end{cases} \tag{8}$$

$$\sum_{k \in \mathcal{K}} a_k \leq M. \tag{9}$$

At the BS, the transmit signal vector $\mathbf{x} \in \mathbb{C}^{N \times 1}$ is expressed as

$$\mathbf{x} = \sum_{k=1}^{K} a_k \mathbf{w}_k s_k, \tag{10}$$

where s_k is the transmit symbol for the k-th user with zero mean and unit variance, and $\mathbf{w}_k$ is a beamforming vector for the k-th user satisfying the power constraint as $\sum_{k=1}^{K} \|\mathbf{w}_k\|^2 a_k \leq P$ with maximum transmit power P. In each coherence block time, the received signal of the k-th user can be expressed as [1]

$$y_k = \left(\mathbf{h}_{d,k}^{\mathsf{H}} + \sum_{l=1}^{L} \mathbf{f}_{l,k}^{\mathsf{H}} \mathbf{\Theta}_l \mathbf{G}_l \right) \sum_{k=1}^{K} a_k \mathbf{w}_k s_k + n_k, \tag{11}$$

where n_k denotes the additive white gaussian noise (AWGN) with zero mean and variance of σ^2. Based on (11), we define the downlink signal-to-interference-plus-ratio (SINR) of the k-th user as

$$\gamma_k = \frac{a_k \left| \left(\mathbf{h}_{d,k}^{\mathsf{H}} + \sum_{l=1}^{L} \mathbf{f}_{l,k}^{\mathsf{H}} \mathbf{\Theta}_l \mathbf{G}_l \right) \mathbf{w}_k \right|^2}{\sum_{i=1, i \neq k}^{K} a_i \left| \left(\mathbf{h}_{d,k}^{\mathsf{H}} + \sum_{l=1}^{L} \mathbf{f}_{l,k}^{\mathsf{H}} \mathbf{\Theta}_l \mathbf{G}_l \right) \mathbf{w}_i \right|^2 + \sigma^2}, \tag{12}$$

Accordingly, the achievable data rate of the k-th user is given as

$$R_k = \log_2 (1 + \gamma_k). \tag{13}$$

III. Problem Formulation and Reformulation

In this section, we focus on formulating the optimization problem to find the optimal solutions of BS beamforming, IRS reflection coefficients and user selection variables. Consider the case that there are more users than the number of antennas at BS, that is, M, we need to select M number of users based on a certain performance criterion, where we consider the sum rate. Also, since the downlink SINR of a user depends on the set of selected users, BS beamforming for other users and IRS reflection coefficients, it is important and meaningful to jointly optimize these variables. Next we present a problem formulation that captures this joint optimization, then employ several reformulation methods to successively make the problem more tractable.

A. Problem Formulation

We aim at maximizing the weighted sum rate of selected users by jointly optimizing the BS transmit beamforming vectors, $\mathbf{w}_k$, the IRS reflection coefficients, $\mathbf{\Theta}_l$, and the user selection variables, a_k. Then, the optimization problem can be formulated as

$$(\mathrm{P1}) \quad \max_{\mathbf{w}_k, \mathbf{\Theta}_l, a_k} \sum_{k=1}^{K} w_k R_k \tag{14a}$$

$$\text{s.t.} \sum_{k=1}^{K} \|\mathbf{w}_k\|^2 a_k \leq P, \ k \in \mathcal{K} \tag{14b}$$

$$\sum_{k=1}^{K} a_k \leq M, \ k \in \mathcal{K} \tag{14c}$$

$$a_k \in \{0, 1\}, \ k \in \mathcal{K} \tag{14d}$$

$$|\theta_{l,n}| = 1, \ l \in \mathcal{L}, \ n \in \mathcal{N} \tag{14e}$$

The sum rate optimization problem can be obtained by setting $w_k = 1$ in problem (P1). When considering proportional fairness between users, we set $w_k = \frac{1}{T_k}$, where T_k is the long term average rate achieved by the k-th user [26]. The constraint (14b) in (P1) denotes the maximum transmit power constraint for BS. The constraint (14c) indicates that BS can select up to M users and (14d) indicates the user selection variable is binary. Lastly, the constraint (14e) indicates that the reflection coefficient of each element has a unit modulus value. Since optimization variables are highly coupled at the objective function with the discrete variable $\{a_k, k \in \mathcal{K}\}$ and a non-convex constraint (14e), this problem is a non-convex mixed integer non-linear

[1] It is worth noting that double/multi-hop reflections between IRSs can also occur in a multi-IRS environment for the reflected signal from a BS to a user. To overcome severe multiplicative path loss in multi-hop reflections, strategically deploying large-scale IRSs to establish LoS links between IRSs or installing active IRSs such as in [25] can offer a performance-enhancing solution. Our current work, however, focuses on passive IRSs which are vulnerable to multi-hop reflections because of the severe attenuation. Therefore, it is reasonable to assume single-reflection links in our case, ignoring multi-reflections between IRSs.

Authorized licensed use limited to: Univ Of Incheon. Downloaded on October 26,2026 at 13:11:01 UTC from IEEE Xplore. Restrictions apply.

programming (MINLP), which is NP-hard and difficult to solve in general. Although an exhaustive search can be used to solve the problem (P1), this incurs prohibitive complexity and is practically infeasible.

In an IRS-aided system, the channel gains are dependent on the IRS reflection coefficients as shown in (11). Thus, it is not possible to select M users with pair-wise orthogonal channels as in [18], since orthogonal users keep changing at the adjustment of IRS reflection coefficients. In this article, we propose a user selection algorithm which adaptively chooses users with the consideration of IRS reflection coefficients.

B. Reformulation With Weighted l_1-Norm Approximation

In this subsection, we reformulate the problem (P1) into a more tractable form by using the relationship between the variables $\mathbf{w}_k$ and a_k. For the design of beamforming vectors at BS, the selected users are supported by BS while other users does not receive any information from BS, which implicitly implies that $\|\mathbf{w}_k\|^2 \geq 0$ if $a_k = 1$ and $\|\mathbf{w}_k\|^2 = 0$, otherwise. Accordingly, the problem (P1) can be reformulated into an equivalent problem as

$$(\text{P1.1}) \quad \max_{\mathbf{w}_k, \mathbf{\Theta}_j} f_1(\mathbf{w}_k, \mathbf{\Theta}_l) = \sum_{k=1}^{K} w_k R_k \tag{15a}$$

$$\text{s.t.} \sum_{k=1}^{K} \|\mathbf{w}_k\|^2 \leq P, \ k \in \mathcal{K} \tag{15b}$$

$$\sum_{k=1}^{K} \mathbb{1}_{\{\|\mathbf{w}_k\|^2\}} \leq M, \ k \in \mathcal{K} \tag{15c}$$

$$|\theta_{l,n}| = 1, \ l \in \mathcal{L}, \ n \in \mathcal{N} \tag{15d}$$

where $\mathbb{1}_{\{x\}}$ is indicator function where $\mathbb{1}_{\{x\}} = 1$ for $x > 0$ and $\mathbb{1}_{\{x\}} = 0$, otherwise. Note that l_0-norm is defined as the total number of nonzero elements in a vector, and thus indicator function in (15c) can be rewritten as

$$\mathbb{1}_{\{\|\mathbf{w}_k\|^2\}} = \left|\|\mathbf{w}_k\|^2\right|_0, \tag{16}$$

Then, the downlink SINR of the k-th user can be rewritten as

$$\gamma_k = \frac{|\left(\mathbf{h}_{d,k}^{\mathsf{H}} + \sum_{l=1}^{L} \mathbf{f}_{l,k}^{\mathsf{H}} \mathbf{\Theta}_l \mathbf{G}_l\right) \mathbf{w}_k|^2}{\sum_{i=1, i\neq k}^{K} |\left(\mathbf{h}_{d,k}^{\mathsf{H}} + \sum_{l=1}^{L} \mathbf{f}_{l,k}^{\mathsf{H}} \mathbf{\Theta}_l \mathbf{G}_l\right) \mathbf{w}_i|^2 + \sigma^2}. \tag{17}$$

Note that we implicitly represent a_k with $\mathbf{w}_k$ in (P1.1). Then we simplify the problem to optimize only two variables $\mathbf{w}_k$ and $\mathbf{\Theta}_l$. However, a major challenge in solving the problem is to handle non-smooth function in (15c). To deal with this challenge, we bring an idea from spatial signal recovery works [21], [27], [28] which approximate a non-convex l_0-norm to a convex weighted l_1-norm as follows

$$|\mathbf{y}|_0 \backsimeq \sum_{m} \mu_m y_m = |\boldsymbol{\mu}^{\mathsf{T}} \mathbf{y}|_1, \tag{18}$$

where y_m is the m-th element of $\mathbf{y}$ and μ_m is a positive weight respect to y_m. For accurate approximation in (18), it is important to choose proper weight $\boldsymbol{\mu}$ while one weight is required for our problem because $\mathbf{y} = \|\mathbf{w}_k\|^2$ has a scalar value. Then, we can relax constraint (15c) as

$$\sum_{k=1}^{K} \mu_k \|\mathbf{w}_k\|^2 \leq M, \ k \in \mathcal{K}, \tag{19}$$

where μ_k is a positive weight for $\|\mathbf{w}_k\|^2$. The appropriate weight to satisfy the approximation (19) is given at the i-th iteration as

$$\mu_k^{i+1} = \frac{1}{\|\mathbf{w}_k^i\|^2 + \varepsilon}, \ k \in \mathcal{K}. \tag{20}$$

where $\varepsilon > 0$ provides stability and needs to be set as a slightly smaller value than the expectation of $\|\mathbf{w}_k\|^2$, i.e., the average transmit power for the selected users [27]. Note that by setting the weight in (20) which is inversely proportional to the power for each user, the smaller value of $\|\mathbf{w}_k^i\|^2$ is, we obtain the higher weight. The users with higher weight would not be selected to satisfy the constraint (19).

Based on (18) and (19), we can formulate the approximated problem of (P1.1) as

$$(\text{P2}) \quad \max_{\mathbf{w}_k, \mathbf{\Theta}_j} f_1(\mathbf{w}_k, \mathbf{\Theta}_l) \tag{21a}$$

$$\text{s.t.} \, (15\text{b}), (15\text{ d}), (19) \tag{21b}$$

We remark that by removing the integer variable for user selection and approximating it into an l_1-norm constraint, this weighted l_1-norm approximation approach achieves lower complexity compared to existing penalty-based iterative relaxation methods [29]. In spite of relaxing (15c) to (19), the non-convex objective function (21a) and non-convex constraint (15d) make the problem difficult to jointly find the optimal solutions of $\mathbf{w}_k$ and $\mathbf{\Theta}_l$. In the following subsection, we reformulate the problem (P2) with using a FP method to deal with these difficulties.

C. Reformulation of (P2) With the FP Method

In this subsection, we aim to reformulate problem (P2) by using the FP method. To address the summation of the logarithmic function in (21a), we use a Largangian dual transform FP technique proposed in [30]. Specifically, by introducing an auxiliary variable $\boldsymbol{\eta} = [\eta_1, \ldots, \eta_K]^{\mathsf{T}} \in \mathbb{R}^{K\times 1}$, the problem (P2) is equivalently reformulated as

$$(\text{P2.1}) \quad \max_{\boldsymbol{\eta}, \mathbf{w}_k, \mathbf{\Theta}_l} f_2(\boldsymbol{\eta}, \mathbf{w}_k, \mathbf{\Theta}_l) \tag{22a}$$

$$\text{s.t.} \quad (15\text{b}), (15\text{ d}), (19) \tag{22b}$$

where the transformed object function $f_2(\boldsymbol{\eta}, \mathbf{w}_k, \mathbf{\Theta}_l)$ is

$$f_2(\boldsymbol{\eta}, \mathbf{w}_k, \mathbf{\Theta}_l) = \sum_{k=1}^{K} w_k \log_2(1+\eta_k) - \sum_{k=1}^{K} w_k \eta_k + \sum_{k=1}^{K} \frac{w_k(1+\eta_k)\gamma_k}{1+\gamma_k}. \tag{23}$$

We note that γ_k in (23) is not in the logarithmic function, which makes the problem more tractable. However, the optimization variables $\boldsymbol{\eta}, \mathbf{w}_k$ and $\mathbf{\Theta}_l$ are still highly coupled. To

Authorized licensed use limited to: Univ Of Incheon. Downloaded on October 26,2026 at 13:11:01 UTC from IEEE Xplore. Restrictions apply.

tackle such difficulties, we utilize the BCD method to alternately update them by solving each subproblem until $f_2(\boldsymbol{\eta}, \mathbf{w}_k, \boldsymbol{\Theta}_l)$ converges.

When $\mathbf{w}_k$ and $\boldsymbol{\Theta}_l$ are fixed, we can easily show that f_2 in (23) is concave to $\boldsymbol{\eta}$. Therefore, the optimal $\boldsymbol{\eta}$ is derived by solving the first-order condition, i.e., $\partial f_2/\partial \eta_k = 0$ for $k \in \mathcal{K}$ and this solution can be given by

$$\eta_k^{\text{opt}} = \gamma_k, \ k \in \mathcal{K}. \tag{24}$$

In the following sections, algorithms which update $\mathbf{w}_k$ and $\boldsymbol{\Theta}_l$ with fixing other variables are presented.

IV. Joint BS Beamforming Design and User Selection

In this section, we optimize the BS beamforming and user selection. First, by fixing $\boldsymbol{\eta}$ and $\boldsymbol{\Theta}_l$, and then introducing auxiliary variables, we transform the problem (P2.1) to a more tractable form with a quadratic transform FP method [31]. Then, we decouple the transformed problem into two subproblems which can be alternately optimized by the BCD method using two alternate steps: 1) updating auxiliary variable, 2) joint BS beamforming and user selection optimization problem. For optimizing the BS beamforming and user selection, a Lagrangian-based subgradient method is proposed.

A. Reformulation of (P2.1) With Fixed $\boldsymbol{\xi}$ and $\boldsymbol{\Theta}_l$

When $\boldsymbol{\eta}$ and $\boldsymbol{\Theta}_l$ are fixed, we only need to consider the last term in the right-hand side from (23) to optimize $\mathbf{w}_k$. Then, the subproblem corresponding to BS beamforming which contains the implicit user scheduling is expressed as

$$(\text{P3}) \quad \max_{\mathbf{w}_k} \ f_{3a}(\mathbf{w}_k) = \sum_{k=1}^{K} \frac{\tilde{\eta_k} |\mathbf{h}_k^{\mathsf{H}} \mathbf{w}_k|^2}{\sum_{i=1}^{K} |\mathbf{h}_k^{\mathsf{H}} \mathbf{w}_i|^2 + \sigma^2} \tag{25a}$$

$$\text{s.t.} \quad (15\text{b}), (15\text{d}) \tag{25b}$$

where $\mathbf{h}_k = \mathbf{h}_{d,k} + \sum_{l=1}^{L} \mathbf{G}_l^{\mathsf{H}} \boldsymbol{\Theta}_l \mathbf{f}_{l,k}$ and $\tilde{\eta_k} = w_k(1+\eta_k)$. However, it is difficult to solve the problem (P3) because of a non-convex sum-of-ratio objective function. To tackle this difficulty, we bring a quadratic transform FP technique proposed in [31]. Specifically, by introducing an auxiliary variable $\boldsymbol{\xi} = [\xi_1, \ldots, \xi_K]^{\mathsf{T}} \in \mathbb{C}^{K \times 1}$, the objective function (25a) is equivalently reformulated as

$$f_{3b}(\boldsymbol{\xi}, \mathbf{w}_k) = \sum_{k=1}^{K} 2\sqrt{\tilde{\eta_k}} \, \text{Re}\left\{\xi_k^* \mathbf{h}_k^{\mathsf{H}} \mathbf{w}_k\right\} - \sum_{k=1}^{K} |\xi_k|^2 \left(\sum_{i=1}^{K} |\mathbf{h}_k^{\mathsf{H}} \mathbf{w}_i|^2 + \sigma^2\right). \tag{26}$$

Note that since the objective function (26) is a convex in terms of $\mathbf{w}_k$, the problem (P3) can be transformed into convex problem. From this reformulated problem, we need to address two variables $\boldsymbol{\xi}$ and $\mathbf{w}_k$ and the alternative updating of these variables are presented in the following subsections.

B. Update Auxiliary Variable $\boldsymbol{\xi}$

For the problem for $\boldsymbol{\xi}$ with fixed $\mathbf{w}_k$, the optimal $\boldsymbol{\xi}$ can be derived by solving the first-order condition, i.e., $\partial f_{3b}/\partial \xi_k = 0$ for $k \in \mathcal{K}$, since $f_{3b}(\boldsymbol{\xi}, \mathbf{w}_k)$ with fixed $\mathbf{w}_k$ is concave to $\boldsymbol{\xi}$, and this solution is obtained by

$$\xi_k^{\text{opt}} = \frac{\sqrt{\tilde{\eta_k}} \mathbf{h}_k^{\mathsf{H}} \mathbf{w}_k}{\sum_{i=1}^{K} |\mathbf{h}_k^{\mathsf{H}} \mathbf{w}_i|^2 + \sigma^2}, \ k \in \mathcal{K}. \tag{27}$$

C. Update Joint BS Beamforming and User Selection $\mathbf{w}_k$

To obtain the optimal $\mathbf{w}_k$ with fixed $\boldsymbol{\xi}$, we first define $\bar{\mathbf{w}} = [\mathbf{w}_1^{\mathsf{H}}, \ldots, \mathbf{w}_K^{\mathsf{H}}]^{\mathsf{H}} \in \mathbb{C}^{MK \times 1}$. Then, the problem (P3) with given $\boldsymbol{\xi}$ is reformulated as the quadratic form given by

$$(\text{P3.1}) \quad \min_{\bar{\mathbf{w}}} \ f_{3c}(\bar{\mathbf{w}}) = \bar{\mathbf{w}}^{\mathsf{H}} \mathbf{A} \bar{\mathbf{w}} - 2\,\text{Re}\left\{\bar{\mathbf{w}}^{\mathsf{H}} \mathbf{h}\right\} + c_1 \tag{28a}$$

$$\text{s.t.} \quad \|\bar{\mathbf{w}}\|^2 \le P \tag{28b}$$

$$\bar{\mathbf{w}}^{\mathsf{H}} \mathbf{M} \bar{\mathbf{w}} \le M \tag{28c}$$

where

$$\mathbf{A} = \mathbf{I}_K \otimes \left(\sum_{k=1}^{K} |\xi_k|^2 \mathbf{h}_k^{\mathsf{H}} \mathbf{h}_k\right), \tag{29}$$

$$\mathbf{h} = \left[\sqrt{\tilde{\eta_1}} \xi_1 \mathbf{h}_1^{\mathsf{H}}, \ldots, \sqrt{\tilde{\eta_K}} \xi_K \mathbf{h}_K^{\mathsf{H}}\right]^{\mathsf{H}}, \tag{30}$$

$$\mathbf{M} = \text{diag}(\mu_1, \ldots, \mu_K) \otimes \mathbf{I}_M, \tag{31}$$

$$c_1 = \sum_{k=1}^{K} |\xi_k|^2 \sigma^2. \tag{32}$$

Note that $\mathbf{A}$ and $\mathbf{M}$ are positive semi-definite matrices, and thus the problem (P3.1) is a convex quadratically constrained quadratic programming (QCQP) which can be solved by the conventional convex optimization tools such as interior point method [32]. However, many users deployed in a crowded hotspot produces a prohibitive complexity to obtain the solution in the problem (P3.1) since the computation complexity of convex optimization is exponentially increased by the order of the number of users. To reduce this complexity, we adopt the Lagrangian duality approach which provides the optimal solution satisfying the strong duality for the convex problem as in (P3.1).

For the Lagrangian duality, we first introduce the dual variables $\lambda \ge 0$ and $\upsilon \ge 0$ to incorporate the constraints (28b) and (28c). Then, the Lagrangian function can be written as

$$L(\bar{\mathbf{w}}, \lambda, \upsilon) = \bar{\mathbf{w}}^{\mathsf{H}} \mathbf{A} \bar{\mathbf{w}} - 2\,\text{Re}\left\{\bar{\mathbf{w}}^{\mathsf{H}} \mathbf{h}\right\} + \lambda\left(\bar{\mathbf{w}}^{\mathsf{H}} \bar{\mathbf{w}} - P\right) + \upsilon\left(\bar{\mathbf{w}}^{\mathsf{H}} \mathbf{M} \bar{\mathbf{w}} - M\right) + c_1 \tag{33}$$

Accordingly, a Lagrangian dual problem is formulated as

$$\max_{\lambda, \upsilon} \ g(\lambda, \upsilon) \quad \text{s.t.} \ \lambda, \upsilon \ge 0 \tag{34}$$

where dual function $g(\lambda, \upsilon)$ is defined as

$$g(\lambda, \upsilon) = \min_{\bar{\mathbf{w}}} L(\bar{\mathbf{w}}, \lambda, \upsilon) \tag{35}$$

Authorized licensed use limited to: Univ Of Incheon. Downloaded on October 26,2026 at 13:11:01 UTC from IEEE Xplore. Restrictions apply.

Algorithm 1: Lagrangian-Based Joint BS Beamforming and User Selection.

1: Initialize $T_{\max}$ and dual variables λ^0, υ^0
2: Set $t = 0$
3: **repeat**
4: Calculate the optimal BS beamformer $\bar{\mathbf{w}}^{\text{opt}}$ by using (36)
5: Update λ^{t+1} and υ^{t+1} by using (37), (38)
6: Set $t = t + 1$
7: **until** f_{3c} converges or $t = T_{\max}$

The obtaining solution in Lagrangian dual problem can be divided into two stages. First, we solve the inner problem (35) about $\bar{\mathbf{w}}$ when the dual variables λ and υ are given. Second, we update λ and υ by solving the outer problem (34) when the primal variable $\bar{\mathbf{w}}$ is given. These variables are iteratively updated until the convergence condition is satisfied.

In the inner problem, by setting the first-order derivative of $L(\bar{\mathbf{w}}, \lambda, \upsilon)$ with respect to $\bar{\mathbf{w}}$ to zero, i.e., $\nabla_{\bar{\mathbf{w}}} L(\bar{\mathbf{w}}, \lambda, \upsilon) = 0$, we can obtain the optimal beamforming vector $\bar{\mathbf{w}}$ as

$$\bar{\mathbf{w}}^{\text{opt}}(\lambda, \upsilon) = \left(\left(\mathbf{A} + \upsilon \mathbf{M} + \lambda \mathbf{I}_{MK} \right)^{\mathsf{H}} \right)^{-1} \mathbf{h}. \tag{36}$$

In the outer problem, we adopt a subgradient method [33] to update λ and υ over each iteration which is given as

$$\lambda^{t+1} = \left[\lambda^t - \delta_1^t \left(P - \| \bar{\mathbf{w}}^{\text{opt}}(\lambda^t, \upsilon^t) \|^2 \right) \right]^+, \tag{37}$$

$$\upsilon^{t+1} = \left[\upsilon^t - \delta_2^t \left(M - \bar{\mathbf{w}}^{\text{opt}}(\lambda^t, \upsilon^t)^{\mathsf{H}} \mathbf{M} \bar{\mathbf{w}}^{\text{opt}}(\lambda^t, \upsilon^t) \right) \right]^+, \tag{38}$$

where δ_1^t and δ_2^t represent positive step size at the t-th iteration[2]. Based on (36)–(38), we summarize our proposed algorithm in Algorithm 1 in detail.

V. IRS Reflection Coefficients Desgin Algorithm

In this section, we optimize the IRS reflection coefficients. First, by fixing $\boldsymbol{\eta}$ and $\mathbf{w}_k$, and then introducing auxiliary variables as in the quadratic transform FP method, we transform problem (P2.1) into a more tractable problem and solve it using an algorithm with two alternating steps: 1) updating auxiliary variable, 2) IRS reflection coefficients. For the step of optimizing the IRS reflection coefficients, we propose a complex circle manifold (CCM) method.

A. Reformulation of (P2.1) With Fixed $\boldsymbol{\xi}$ and $\mathbf{w}_k$

In Sections III and IV, we optimized both variables $\boldsymbol{\eta}$ and $\mathbf{w}_k$ where $\boldsymbol{\eta}$ and $\mathbf{w}_k$ are obtained by (24) and Algorithm 1. When these variables are fixed, we only need to consider the last term in (23) to optimize $\boldsymbol{\Theta}_l$. By denoting $\mathbf{u}_l = [\theta_{l,1}, \ldots, \theta_{l,N}]^{\mathsf{H}}$, $\mathbf{u} = [\mathbf{u}_1^{\mathsf{H}}, \ldots, \mathbf{u}_L^{\mathsf{H}}]^{\mathsf{H}} \in \mathbb{C}^{NL \times 1}$, $\mathbf{B}_{l,k} = \text{diag}(\mathbf{f}_{l,k}^{\mathsf{H}}) \mathbf{G}_l$, $\mathbf{d}_{k,i} = [\mathbf{w}_i^{\mathsf{H}} \mathbf{B}_{1,k}^{\mathsf{H}}, \ldots, \mathbf{w}_i^{\mathsf{H}} \mathbf{B}_{L,k}^{\mathsf{H}}]^{\mathsf{H}} \in \mathbb{C}^{NL \times 1}$ and $e_{k,i} = \mathbf{h}_{d,k}^{\mathsf{H}} \mathbf{w}_i$, the subproblem corresponding to IRS reflection coefficients is expressed as

$$(\text{P4}) \quad \max_{\mathbf{u}} \quad f_{4a}(\mathbf{u}), \tag{39a}$$

$$\text{s.t.} \quad (15\,\text{d}) \tag{39b}$$

where the objective function $f_{4a}(\mathbf{u})$ is written as

$$f_{4a}(\mathbf{u}) = \sum_{k=1}^{K} \frac{\tilde{\eta_k} |e_{k,k} + \mathbf{u}^{\mathsf{H}} \mathbf{d}_{k,k}|^2}{\sum_{i=1}^{K} |e_{k,i} + \mathbf{u}^{\mathsf{H}} \mathbf{d}_{k,i}|^2 + \sigma^2}. \tag{40}$$

Note that since (40) is the form of the summation of ratio function, we can also apply the quadratic transform FP technique in Section IV. Specifically, by introducing an auxiliary variable $\boldsymbol{\rho} = [\rho_1, \ldots, \rho_K]^{\mathsf{T}} \in \mathbb{C}^{K \times 1}$, the problem (P4) is equivalently reformulated as

$$(\text{P4.1}) \quad \max_{\boldsymbol{\rho}, \mathbf{u}} \; f_{4b}(\boldsymbol{\rho}, \mathbf{u})$$

$$= \sum_{k=1}^{K} 2 \sqrt{\tilde{\eta_k}} \, \text{Re} \left\{ \rho_k^* \left(e_{k,k} + \mathbf{u}^{\mathsf{H}} \mathbf{d}_{k,k} \right) \right\} - \sum_{k=1}^{K} |\rho_k|^2 \left(\sum_{i=1}^{K} |e_{k,i} + \mathbf{u}^{\mathsf{H}} \mathbf{d}_{k,i}|^2 + \sigma^2 \right). \tag{41a}$$

$$\text{s.t.} \quad (15\text{e}) \tag{41b}$$

Similar to the procedure in Section IV, the problem (P4.1) can be solved by two steps where $\boldsymbol{\rho}$ and $\mathbf{u}$ are alternatively solved by fixing another variable which are described in the following subsections.

B. Update Auxiliary Variable $\boldsymbol{\rho}$

For the problem for $\boldsymbol{\rho}$ with fixed $\mathbf{u}$, the optimal $\boldsymbol{\rho}$ can be derived by solving the first-order condition, i.e., $\partial f_{4b} / \partial \rho_k = 0$ for $k \in \mathcal{K}$, since $f_{4b}(\boldsymbol{\rho}, \mathbf{u})$ with fixed $\mathbf{u}$ is concave to $\boldsymbol{\rho}$, and this solution can be obtained by

$$\rho_k^{\text{opt}} = \frac{\sqrt{\tilde{\eta_k}} \left(e_{k,k} + \mathbf{u}^{\mathsf{H}} \mathbf{d}_{k,k} \right)}{\sum_{i=1}^{K} |e_{k,i} + \mathbf{u}^{\mathsf{H}} \mathbf{d}_{k,i}|^2 + \sigma^2}, \; k \in \mathcal{K}. \tag{42}$$

C. Update IRS Reflection Coefficients $\mathbf{u}$

After reorganizing (41a), the problem (P4.1) with given $\boldsymbol{\rho}$ can be simply expressed as

$$(\text{P4.2}) \quad \min_{\mathbf{u}} \quad f_{4c}(\mathbf{u}) = \mathbf{u}^{\mathsf{H}} \mathbf{Q} \mathbf{u} + 2 \, \text{Re} \left\{ \mathbf{u}^{\mathsf{H}} \mathbf{r} \right\} + c_2 \tag{43a}$$

$$\text{s.t.} \quad (15\text{e}) \tag{43b}$$

where

$$\mathbf{Q} = \sum_{k=1}^{K} \sum_{i=1}^{K} |\rho_k|^2 \mathbf{d}_{k,i} \mathbf{d}_{k,i}^{\mathsf{H}}, \tag{44}$$

$$\mathbf{r} = \sum_{k=1}^{K} \left(\sum_{i=1}^{K} |\rho_k|^2 e_{k,i}^* \mathbf{d}_{k,i} - \sqrt{\tilde{\eta_k}} \, \text{Re} \left\{ \rho_k^* \mathbf{d}_{k,k} \right\} \right), \tag{45}$$

[2]Constant or square summable but not summable step size rules can be used in (37), (38) [33].

Authorized licensed use limited to: Univ Of Incheon. Downloaded on October 26,2026 at 13:11:01 UTC from IEEE Xplore. Restrictions apply.

Algorithm 2: CCM-Based IRS Reflection Coefficients Design

1: Initialize $T_{\max}$ and $\mathbf{u}^0$
2: Set $t = 0$
3: **repeat**
4: Calculate the search direction in Euclidean Space $\boldsymbol{\zeta}^t$ by using (49)
5: Calculate the Riemannian gradient $\mathbf{P}_{\mathcal{T}_{\mathbf{u}^t}\mathcal{M}}(\boldsymbol{\zeta}^t)$ by using (50)
6: Update $\hat{\mathbf{u}}^t$ on tangent space by using (51)
7: Update $\mathbf{u}^{t+1}$ with retraction by using (53)
8: Set $t = t + 1$
9: **until** f_{4c} converges or $t = T_{\max}$

$$c_2 = \sum_{k=1}^{K}\left(\sum_{i=1}^{K}|\rho_k|^2\left(|e_{k,i}|^2+\sigma^2\right) - \sqrt{\tilde{\eta_k}}\,\mathrm{Re}\left\{\rho_k^* e_{k,k}\right\}\right). \tag{46}$$

We here point out that the objective function (43a) is a convex since $\mathbf{Q}$ is a positive semi-definite matrix. However, the unit modulus constraint (43b) is still non-convex and various techniques to handle this non-convexity have been considered such as SDR and penalty CCA [3], [34]. These methods can transform the constraint (43b) into convex but do not guarantee a satisfactory performance and fast convergence at a reasonable complexity [35]. Therefore, we adopt a complex circle manifold (CCM) method which performs well with a relatively low complexity [36], [37].

In this method, we can first express the constraint (43b) as a following feasible set

$$\mathcal{M} = \left\{\mathbf{u} \in \mathbb{C}^{NL\times 1} : |u_p| = 1, p = 1, \ldots, NL\right\}, \tag{47}$$

where (47) can be seen as a product of NL complex circle and a sub-manifold of $\mathbb{C}^{NL\times 1}$. This is generally known as a complex circle manifold. Then, we can equivalently transform the problem as

$$(\mathrm{P4.3}) \min_{\mathbf{u}\in\mathcal{M}} \; f_{4c}(\mathbf{u}) = \mathbf{u}^{\mathsf{H}}\left(\mathbf{Q}+\omega\mathbf{I}_{NL}\right)\mathbf{u} + 2\,\mathrm{Re}\left\{\mathbf{u}^{\mathsf{H}}\mathbf{r}\right\} + c_2, \tag{48}$$

where ω is a positive parameter to control a convergence and does not impact on the optimal solution since $\omega\mathbf{u}^{\mathsf{H}}\mathbf{u} = \omega NL$ is a constant value. For convergence, this parameter needs to satisfy the condition, $\omega \geq \frac{NL}{8}\lambda_{\mathbf{Q}} + \|\mathbf{r}\|^2$, where $\lambda_{\mathbf{Q}}$ is a maximum eigenvalue of $\mathbf{Q}$ [36, Lemma 3.2]. Similar to a gradient descent which is a simple line search method over Euclidean space to find a solution in a nonlinear unconstrained convex problem, the main concept of CCM method is to apply gradient descent in the region of manifold $\mathcal{M}$. For this algorithm, the following four steps at each iteration t can be applied:

1) Search Direction in Euclidean Space: First, we need to compute a search direction in Euclidean space. At $\mathbf{u}^t$, a negative gradient of the objective function $f_{4c}(\mathbf{u})$ is the most common and steepest search direction. This is expressed as

$$\boldsymbol{\zeta}^t = -\nabla_{\mathbf{u}} f_{4c}(\mathbf{u})\big|_{\mathbf{u}=\mathbf{u}^t} = -2\left(\mathbf{Q}+\omega\mathbf{I}_{NL}\right)\mathbf{u}^t - 2\mathbf{r} \tag{49}$$

2) Project to Tangent Space $\mathcal{T}_{\mathbf{u}^t}\mathcal{M}$: Second, we need to find a search direction in manifold $\mathcal{M}$ which is called Riemannian gradient since line searching must be performed in manifold itself not in Euclidean space. In details, Riemannian gradient at $\mathbf{u}^t$ can be computed by projecting $\boldsymbol{\zeta}^t$ onto the tangent space of $\mathcal{M}$ at $\mathbf{u}^t$, i.e., $\mathcal{T}_{\mathbf{u}^t}\mathcal{M}$. We can express this process as

$$\mathbf{P}_{\mathcal{T}_{\mathbf{u}^t}\mathcal{M}}(\boldsymbol{\zeta}^t) = \boldsymbol{\zeta}^t - \mathrm{Re}\left\{\boldsymbol{\zeta}^{t*}\odot\mathbf{u}^t\right\}\odot\mathbf{u}^t \tag{50}$$

3) Update $\mathbf{u}^t$ on Tangent Space: Third, we update current $\mathbf{u}^t$ with a direction $\mathbf{P}_{\mathcal{T}_{\mathbf{u}^t}\mathcal{M}}(\boldsymbol{\zeta}^t)$ on the tangent space which is expressed as

$$\hat{\mathbf{u}}^t = \mathbf{u}^t + \delta\,\mathbf{P}_{\mathcal{T}_{\mathbf{u}^t}\mathcal{M}}\left(\boldsymbol{\zeta}^t\right) \tag{51}$$

where δ is a step size. This value should be carefully decided to ensure that the objective function decreases over iterations, and it can be determined by satisfying the following condition [36, Lemma 3.1]

$$0 < \delta < \frac{1}{\lambda_{\mathbf{Q}+\omega\mathbf{I}_{NL}}}. \tag{52}$$

4) Operate the Retraction of $\hat{\mathbf{u}}^t$ to $\mathcal{M}$: Last, we do a retraction operation by mapping obtained $\hat{\mathbf{u}}^t$ onto the manifold $\mathcal{M}$ since the probability of $\hat{\mathbf{u}}^t$ in $\mathcal{M}$ is very low. Specifically, this operation can be expressed as

$$\mathbf{u}^{t+1} = \hat{\mathbf{u}}^t \odot \frac{1}{|\hat{\mathbf{u}}^t|}. \tag{53}$$

The proposed CCM method performs above four steps over every iterations until the objective function f_{4c} converges, which are summarized in Algorithm 2 in detail.

VI. Overall Algorithm and Convergence/Complexity Analysis

A. Summary of the Overall Algorithm

Based on the previous sections, we provide the detailed descriptions of a FP-based optimization framework for solving joint BS beamforming, IRS reflection coefficients, and user selection in Algorithm 3. The original problem is decomposed into the three subproblems of (25), (39), and updating $\boldsymbol{\eta}$. First, in steps 5-6, a process for solving BS beamforming and user selection subproblem is composed of updating $\boldsymbol{\xi}$ as (27) and $\mathbf{w}$ with Lagrangian based algorithm described in Algorithm 1. Second, in steps 7-8, a process for solving IRS reflection coefficients subproblem is composed of updating $\boldsymbol{\rho}$ as (42) and $\mathbf{u}$ with CCM method described in Algorithm 2. Third, $\boldsymbol{\rho}$ can be updated by (24) as in step 9. Last, μ_k can be updated by (20) as in step 10. The algorithm repeats the above steps until the objective function f_1 converges. After convergence, the power for non-selected users is small but is not zero. Hence, we need to employ a threshold to select the users with higher effective gain. In other words, if $\|\mathbf{w}_k\|^2$ is less than the threshold ϵ, then it is set to zero, i.e., $\mathbf{w}_k = \mathbf{0}_M$.

Authorized licensed use limited to: Univ Of Incheon. Downloaded on October 26,2026 at 13:11:01 UTC from IEEE Xplore. Restrictions apply.

Algorithm 3: Joint BS Beamforming, IRS Reflection Coefficients, and User Selection for IRS-Aided Network.

1: Initialize $T_{\max}$, $\mathbf{w}_k$ as MRT beamforming for direct channel, i.e., $\mathbf{w}_k^0 = \sqrt{\frac{P}{K}}\frac{\mathbf{h}_{d,k}}{\|\mathbf{h}_{d,k}\|}$, weight as $\mu_k^0 = \frac{M}{P}$, and reflection coefficients as any feasible $\boldsymbol{\Theta}_l^0$.
2: Set $t = 0$
3: **repeat**
4: Set $t = t + 1$
5: Update $\boldsymbol{\xi}^t$ by using (27)
6: Update $\mathbf{w}^t$ by using Algorithm 1
7: Update $\boldsymbol{\rho}^t$ by using (42)
8: Update $\mathbf{u}^t$ by using Algorithm 2
9: Update $\boldsymbol{\eta}^t$ by using (24)
10: Update μ_k^t by using (20)
11: **until** f_1 converges or $t = T_{\max}$
12: Set $\mathbf{w}_k = \mathbf{0}_{M\times 1}$ if $\|\mathbf{w}_k\|^2 \leq \epsilon_{\text{us}}$

B. Convergence Analysis

In this subsection, we analyze the convergence of proposed Algorithm 3 by verifying that the objective function $f_1(\mathbf{w}_k, \boldsymbol{\Theta}_l)$ is non-decreasing over iterations, as in the following proposition.

Proposition 1 In Algorithm 3, the objective function $f_1(\mathbf{w}_k, \boldsymbol{\Theta}_l)$ is non-decreasing over iterations.

Proof: See Appendix A. □

Furthermore, it is important to note that $f_1(\mathbf{w}_k, \boldsymbol{\Theta}_l)$ is upper bounded by a finite value, due to the limited transmit power of the BS and the finite number of IRSs and reflecting elements. As such, our proposed algorithm converges to a local optimum.

C. Complexity Analysis

In this subsection, we analyze the complexity of the proposed algorithm described in Algorithm 3. In steps 5, 7 and 9, the complexity for updating $\boldsymbol{\xi}$, $\boldsymbol{\rho}$ and $\boldsymbol{\eta}$ is $\mathcal{O}(MK)$, $\mathcal{O}(NLK)$ and $\mathcal{O}(K^2\,M^2)$ [30]. In addition, updating $\mathbf{w}$ in Algorithm 1 requires the complexity of $\mathcal{O}(I_1((MK)^3 + (MK)^2))$ mainly caused by matrix inversion, where I_1 is the total iteration number required in Algorithm 1. In the IRS reflection coefficients optimization in Algorithm 2, the complexity of updating $\mathbf{u}$ is $\mathcal{O}((LN)^3 + I_2(LN)^2)$ where I_2 is the total iteration number required in Algorithm 2 [37]. Therefore, the total complexity of Algorithm 3 is of order $\mathcal{O}(I_3(I_1((MK)^3) + (LN)^3 + I_2(LN)^2))$ where I_3 is a total iteration number required in Algorithm 3.

VII. Low Complexity Algorithms

Although the proposed algorithm in the previous section can jointly optimize the BS beamforming, IRS reflection coefficients, and user selection, its complexity is high due to the large number of users and IRS reflecting elements. This high computational complexity can make the algorithm infeasible in practical systems and motivates us to develop a low complexity algorithm. In this section, we propose two greedy heuristic algorithms and present the detailed descriptions of these algorithms in the following subsections.

A. Correlation Based User Selection Algorithm

The computational complexity in Algorithm 3 is $\mathcal{O}((MK)^3)$ which occurs due to the implicit user selection by optimizing the BS beamforming. This will be impractically high complexity if the number of users is very large, such as in a hotspot area. To deal with this difficulty, in this subsection, we propose an algorithm which first selects highly uncorrelated users, and then jointly designs the beamforming and reflection coefficients with the FP-based BCD method proposed in Algorithm 3. By using a simple metric for user selection, the complexity can be significantly reduced compared to Algorithm 3 with the implicit user selection.

Intuitively, selecting the users with orthogonal channels improves the achievable sum rate by reducing the inter-user interference. If the channels are orthogonal, then BS can transmit signals with a simple linear MRT beamforming which simultaneously maximizes a received power for each user and eliminates inter-user interference. To characterize the channel relationship between users, we adopt the following correlation metric for user selection

$$c_{ki} = \frac{|\mathbf{h}_k^{\mathsf{H}}\mathbf{h}_i|}{\|\mathbf{h}_k\|\|\mathbf{h}_i\|},\ \forall k, i \in \mathcal{K},\ k \neq i \tag{54}$$

where $0 \leq c_{ki} \leq 1$ can be regarded as a magnitude of the correlation coefficient and two channel vectors are close to orthogonal if $c_{ki} \backsimeq 0$. When BS using the MRT beamforming, i.e., $\mathbf{w}_k = \mathbf{h}_k/\|\mathbf{h}_k\|$, the SINR for the k-th user defined in (17) can be re-expressed as

$$\mathsf{SINR}_k = \frac{c_{kk}^2}{\sigma^2/\|\mathbf{h}_k\|^2 + \sum_{i\in\mathcal{K}, i\neq k} c_{ki}^2}. \tag{55}$$

In (55), we can see that selecting the users having high effective channel gain and low correlation with other users is favorable to improving the sum rate performance. Motivated by this, we define the following novel metric for selecting users

$$\Lambda = \sum_{k\in\mathcal{S}} \frac{\|\mathbf{h}_k\|^2}{\sum_{i\in\mathcal{S}, i\neq k} c_{ki}^2}, \tag{56}$$

where $\mathcal{S}$ is the set for selected users with $|\mathcal{S}| \leq M$. Although maximizing Λ can be found by exhaustive search, this brings a huge complexity in the order of $\mathcal{O}(\binom{K}{M})$, which is significantly increased as the number of deployed users increases. To deal with this difficulty, we propose the greedy user selection algorithm which finds the best user to be added to the existing selected user set. The detailed procedure of proposed greedy user selection algorithm is described as follows: First, we initialize the selected user set as $\mathcal{S}_0 = \emptyset$ and the reflection coefficients for each IRS by aligning the phase shifts to the nearest user. Then, at each iteration t, we iteratively update the selected user set as $\mathcal{S}_t = \mathcal{S}_{t-1} \cup \{k_t\}$ by selecting the user $k_t \in \mathcal{K}\backslash\mathcal{S}_{t-1}$ which maximizes the following metric:

$$k_t = \arg\max_{k\in\mathcal{K}\backslash\mathcal{S}_{t-1}} \frac{\|\mathbf{h}_k\|^2}{\sum_{i\in\mathcal{S}_{t-1}} c_{ki}^2}. \tag{57}$$

Authorized licensed use limited to: Univ Of Incheon. Downloaded on October 26,2026 at 13:11:01 UTC from IEEE Xplore. Restrictions apply.

Algorithm 4 Correlation-based User Selection Algorithm

Initialize $\mathcal{S}_0 = \emptyset$ and reflection coefficients for each IRS as phase shifts aligned to nearest user.
for $t = 1$ to M **do**
  if $t = 1$ **then**
    $k_1 = \arg\max_k \|\mathbf{h}_k\|^2$
    $\mathcal{S}_1 = \{k_1\}$
  else
    $k_t = \arg\max_{k \in \mathcal{K} \backslash \mathcal{S}_{t-1}} \frac{\|\mathbf{h}_k\|^2}{\sum_{i \in \mathcal{S}_{t-1}} c_{ki}^2}$
    $\mathcal{S}_t \leftarrow \mathcal{S}_{t-1} \cup \{k_t\}$
  end if
end for
return $\mathcal{S} = \mathcal{S}_M$

This algorithm stops until M users are selected. After selecting all the users, we design the BS beamforming and IRS reflection coefficients using the FP-based BCD method (referred to Algorithm 3) for these selected users where initialization input of $\mathbf{w}_k$ and $\mathbf{\Theta}_l$ are set to the MRT beamforming for effective channel $\mathbf{h}_k$ and reflection coefficients used in the above procedure, respectively. The detailed descriptions of proposed low complexity algorithm are summarized in Algorithm 4.

Complexity Analysis: The major complexity of this proposed algorithm comes from the calculation of (57) which is of order $\mathcal{O}(KN^2\,M^2)$ since the computation of metric (54) requires $\mathcal{O}(N^2\,M^2)$ and it is calculated for all candidate users $\mathcal{K}$. Therefore, the total complexity including the BS beamforming and IRS reflection optimization is given by $\mathcal{O}(KN^2\,M^2 + I_3(I_1((M^2)^3) + (LN)^3 + I_2(LN)^2))$. Note that since the user selection is performed in advance before optimizing the BS beamforming, it converges much faster than Algorithm 3 and can reduce the complexity by decreasing the required iteration numbers.

B. ZF-Based User Selection Algorithm

Since FP-based BS beamforming and IRS reflection coefficients optimization are used in Algorithm 4, its complexity is proportional to N^3 which is still quite high when considering a large number of reflecting elements in general. In this subsection, we propose another low complexity user selection algorithm based on the following two important features. First, each IRS may affect the achievable rate performance mainly for users close to it. Since a cascaded BS-IRS-user channel suffers from double path loss, only IRS located nearby a user can enhance the system performance of that user. Therefore, we only need to design reflection coefficients of each IRS for serving its nearby users, which can reduce the complexity by ignoring the user far away from that IRS. Second, [38] reveals that when aligning IRS's reflection coefficients to only its nearest user with ZF beamforming, the rate of this user can at most scale on the order of $\log_2(N^2)$, while the rate of other users scales at least on the order of $\log_2(N)$. In other words, using ZF beamforming and simply aligning IRS reflection coefficients to a user without optimizing as in Algorithm 2 can improve the overall performance with low computational complexity even if the reflection coefficients of each IRS are aligned for only one user.

Based on the above features of ZF beamforming, we extend the greedy ZF beamforming user selection algorithm developed in [19]. The existing algorithm in [19] selects the user who achieves the maximum sum rate at each iteration with ZF beamforming and water-filling power allocation until the sum rate is no longer increasing or the BS has selected M users. However, since an IRS can change the channel behavior of BS-IRS-user link, this algorithm needs to be modified to update the IRS reflection coefficients while selecting the users with ZF beamforming. This proposed algorithm is composed of the following three steps:

1) Initialization: First, we initialize the selected user group as $\mathcal{S}_0 = \emptyset$. Also, we initialize the IRS reflection coefficients, the aggregated channel and the maximum sum rate as $\mathbf{\Theta}_l = \mathbf{I}_N$, $\mathbf{H}(\mathcal{S}_0) = \emptyset$ and $R_{\max} = 0$, respectively. Each IRS $l, l \in \mathcal{L}$, can be associated with only one user ω_l, such that the phase of its reflected signal is aligned with direct signal at the user. We denote l_k as the index of an associated IRS for the k-th user and assume that each user can be associated with only one IRS providing the highest IRS-user channel gain, i.e., $l_k = \arg\max_l \|\mathbf{f}_{l,k}\|^2$. Also, let $\pi_l(k), k \in \mathcal{K}$ denote the order of the k-th user if IRS l-user channel gains of user set $\mathcal{K}$ are sorted in a descending order.

2) First User Selection: Next, we select the user whose channel gain has the maximum value such that

$$k_1 = \arg\max_{k \in \mathcal{K}} \|\mathbf{h}_k\|^2. \tag{58}$$

For the selected user, the IRS l_{k_1} is associated to support that user, and then its phase shifts are controlled to align the phase of effective direct channel $\mathbf{h}_{d,k_1}^{\mathsf{H}}\mathbf{w}_{k_1}$ to the cascaded channel $\mathbf{f}_{l_{k_1},k_1}^{\mathsf{H}}\mathbf{\Theta}_{l_{k_1}}\mathbf{G}_{l_{k_1}}\mathbf{w}_{k_1}$. Thus, the phase shift of the n-th element at the IRS l_{k_1} is updated by [3]

$$\phi_{l_{k_1},n} = \angle(\mathbf{h}_{d,k_1}^{\mathsf{H}}\mathbf{w}_{k_1}) - \angle\left(f_{l_{k_1},k_1,n}^{*}\right) - \angle\left(\mathbf{g}_{l_{k_1},n}^{\mathsf{H}}\mathbf{w}_{k_1}\right),\ n \in \mathcal{N} \tag{59}$$

where $f_{l_{k_1},k_1,n}^{*}$ is the n-th element of $\mathbf{f}_{l_{k_1},k_1}^{\mathsf{H}}$ and $\mathbf{g}_{l_{k_1},n}^{\mathsf{H}}$ is the n-th row vector of $\mathbf{G}_{l_{k_1}}$. Based on (59), we update $\mathcal{S}_1 \leftarrow \{k_1\}$, $\mathbf{H}(\mathcal{S}_1) = \mathbf{h}_{k_1}^{\mathsf{H}}$, $R_{\max} = R_{k_1}$ and $\omega_{l_{k_1}} = k_1$.

3) Iterative Greedy User Selection: At each iteration $t > 1$, we select the additional user $k_t \in \mathcal{K}\backslash\mathcal{S}_{t-1}$ who achieves the maximum sum rate with ZF beamforming and water-filling power allocation. This problem can be formulated as [19]

$$k_t = \arg\max_{k \in \mathcal{K}\backslash\mathcal{S}_{t-1}} R_{\mathsf{zf}}(\mathcal{S}_{t-1} \cup \{k\}), \tag{60a}$$

$$\text{s.t.} \sum_{i \in \mathcal{S}_{t-1} \cup \{k\}} \left[\tau - \frac{1}{l_i(\mathcal{S}_{t-1} \cup \{k\})}\right]_+ = \frac{P}{\sigma^2} \tag{60b}$$

where

$$R_{\mathsf{zf}}(\mathcal{S}_{t-1} \cup \{k\}) = \sum_{i \in \mathcal{S}_{t-1} \cup \{k\}} \log_2(\tau l_i(\mathcal{S}_{t-1} \cup \{k\})), \tag{61}$$

Authorized licensed use limited to: Univ Of Incheon. Downloaded on October 26,2026 at 13:11:01 UTC from IEEE Xplore. Restrictions apply.

Algorithm 5 ZF-Based User Selection Algorithm

Initialize $\mathcal{S}_0 = \emptyset$, $\mathbf{\Theta}_l = \mathbf{I}_N$, $\mathbf{H}(\mathcal{S}_0) = \emptyset$, $R_{\max} = 0$, and $\pi_l(k), k \in \mathcal{K}$
Set $t = 1$
$k_1 = \arg\max_{k\in\mathcal{K}} \|\mathbf{h}_k\|^2$
$\mathcal{S}_1 \leftarrow \{k_1\}$
Update phase shifts by using (59), $\mathbf{H}(\mathcal{S}_1) = \mathbf{h}_{k_1}^{\mathsf{H}}$, $R_{\max} = R_{k_1}$ and $\omega_{l_{k_1}} = k_1$
while $t < M$ **do**
  $t \leftarrow t + 1$
  Select $k_t \in \mathcal{K}\backslash\mathcal{S}_{t-1}$ in the problem (60)
  if $R_{\mathsf{zf}}(\mathcal{S}_{t-1} \cup \{k_t\}) > R_{\max}$ **then**
    $\mathcal{S}_t \leftarrow \mathcal{S}_{t-1} \cup \{k_t\}$
    if IRS l_{k_t} is not associated with any users or $\pi_{l_{k_t}}(k_t) < \pi_{l_{k_t}}(\omega_{l_{k_t}})$ **then**
      Update $\omega_{l_{k_t}} = k_t$ and phase shifts by using (59)
    end if
    Update $\mathbf{H}(\mathcal{S}_t)$ and $R_{\max} = \sum_{k\in\mathcal{S}_t} R_k$
  else
    $t \leftarrow t - 1$
    break
  end if
end while
Set $\mathbf{w}_k$ with ZF beamforming and water-filling power allocation respect to $\mathbf{H}(\mathcal{S}_t)$
return $\mathcal{S} = \mathcal{S}_t$, $\mathbf{w}_k$ and $\mathbf{\Theta}_l$

$$l_i(\mathcal{S}_{t-1} \cup \{k\}) = \frac{1}{[(\mathbf{H}(\mathcal{S}_{t-1} \cup \{k\})\mathbf{H}(\mathcal{S}_{t-1} \cup \{k\})^{\mathsf{H}})^{-1}]_{i,i}}. \tag{62}$$

In (60), τ is obtained by solving water-filling equation in (60b). After selecting user k_t, we update $\mathcal{S}_t \leftarrow \mathcal{S}_{t-1} \cup \{k_t\}$ if $R_{\mathsf{zf}}(\mathcal{S}_{t-1} \cup \{k_t\}) > R_{\max}$ is satisfied. Also, if IRS l_{k_t} is not associated with any users or $\pi_{l_{k_t}}(k_t) < \pi_{l_{k_t}}(\omega_{l_{k_t}})$, we set $\omega_{l_{k_t}} = k_t$ and align the phase shifts of the IRS l_{k_t} to user k_t similar to (59). Then, we update $\mathbf{H}(\mathcal{S}_t) = [\mathbf{h}_{k_1}, \mathbf{h}_{k_2}, \ldots, \mathbf{h}_{k_t}]^{\mathsf{H}}$ and $R_{\max} = \sum_{k\in\mathcal{S}_t} R_k$. The algorithm is iteratively performed until M users are selected or $R_{\mathsf{zf}}(\mathcal{S}_{t-1} \cup \{k_t\}) > R_{\max}$ is not satisfied. The detailed descriptions of our proposed algorithm are summarized in Algorithm 5.

Complexity Analysis: In this ZF-based user selection algorithm, the user selection with ZF beamforming per iteration has a complexity of $\mathcal{O}(M^2\,K)$ while the complexity of water-filling power allocation is of order $\mathcal{O}(M^2\,K^2)$ [19]. For the update of IRS reflection coefficient in (59) requires a complexity of $\mathcal{O}(MN)$. Therefore, the total complexity of Algorithm 5 is expressed as $\mathcal{O}((M^2K + MN + M^2\,K^2)M)$.

VIII. Performance Evaluation

In this section, we evaluate the performance of our proposed algorithms by simulations. We contrast our algorithms with several benchmark schemes and also analyze the impact of system parameters on algorithm performance.

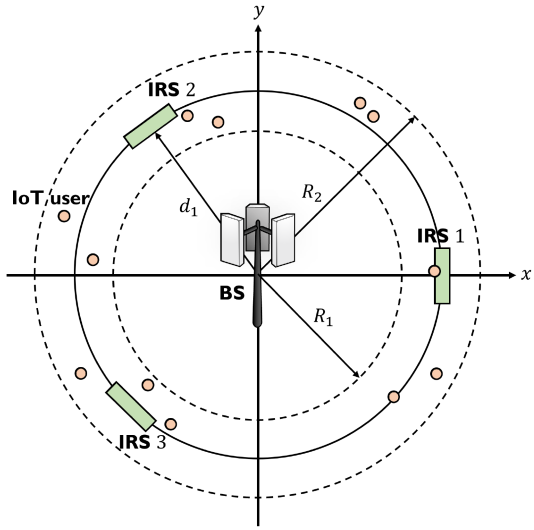


Fig. 2. Illustration of the location of BS, IRSs, and users.

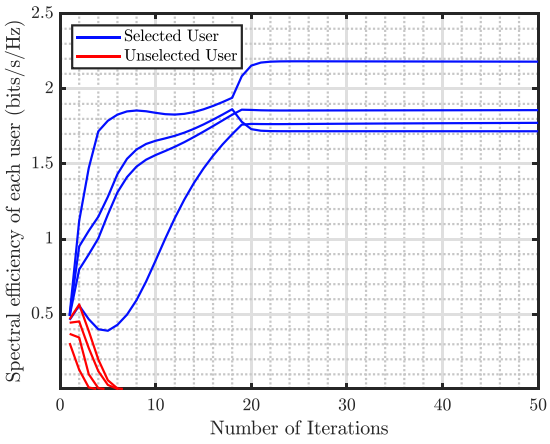
A. Simulation Setups

As illustrated in Fig. 2, we consider a 3-D coordinate single cell network system where BS is located at (0m, 0m, 25m) and the l-th IRS is located at $(d_1(\cos(2\pi l/L))\text{m}, d_1(\sin(2\pi l/L))\text{m}, 10\text{m})$. Also, K users are uniformly distributed in a ring area within radius $[R_1, R_2]$ and the height of all users is set to 0m. Unless specifically specified, for system parameters, we set $M = 8$, $L = 3$, $N = 60$, $N_v = 5$, $K = 30$, $P = 30$ dBm and $\sigma^2 = -85$ dBm. Also, we set $d_1 = 150\text{m}$, $R_1 = 130\text{m}$ and $R_2 = 170\text{m}$, such that users are likely to be located near the IRSs and can benefit from IRS reflections. If users are located within the radius range $[1, 130]\text{m}$, the BS tends to select users who are closer to that BS due to its low path loss and IRS reflections will have little impact for those users. The path loss for the BS-l-th IRS, the l-th IRS-k-th user and the BS-k-th user channels can be modeled by $\alpha_l = 30 + 22\log(d_{1,l})$, $\alpha_{l,k} = 30 + 22\log(d_{2,l,k})$, and $\beta_k = 32.6 + 36.7\log(d_{3,k})$, respectively, where $d_{2,l,k}$, $d_{1,l}$, and $d_{3,k}$ are distance for each corresponding channel. The Rician factors for the BS-IRS link and the IRS-user link are used as $\kappa_{\mathsf{BI}} = 5$dB and $\kappa_{\mathsf{BI}} = 1$dB, respectively. In the simulations, all the results are obtained by averaging over 1500 realization of user location and channels. For the optimization problem, we set the weights of users as $w_k = 1$. All the simulations are performed in Intel i5-9600 K CPU processor with 3.70 GHz and Matlab 2022a.

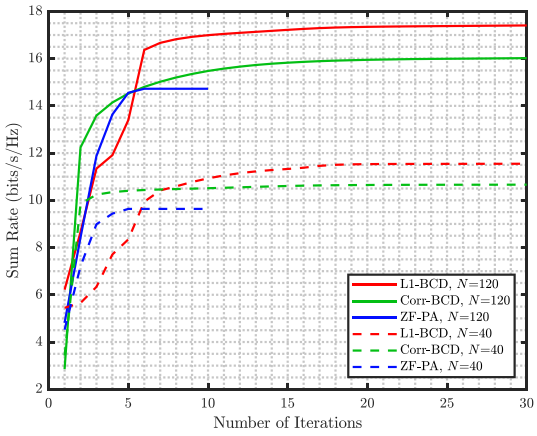
To show the performance gain of our proposed algorithms, we consider the following benchmark schemes:

1) **Random User Selection (RUS)**: M users are randomly selected from K users, while the BS beamforming and IRS reflection coefficients for selected users are jointly designed by the proposed FP-based BCD algorithm.
2) **Single IRS** ($L = 1$): Only a single IRS is deployed in a cell, and the proposed algorithms are applied for designing the BS beamforming, IRS phase shifts, and user selection.
3) **Without IRS (w/o IRS)**: Without IRSs in a cell, the BS beamforming and user selection are jointly designed

Authorized licensed use limited to: Univ Of Incheon. Downloaded on October 26,2026 at 13:11:01 UTC from IEEE Xplore. Restrictions apply.



(a)



(b)

Fig. 3. Sum rate convergence behavior of proposed user selection algorithms. (a) Convergence of the spectral efficiency of each user for $M = 4, L = 3, N = 40, K = 8, P = 30$ dBm. (b) Sum rate for $M = 8, L = 3, K = 30, P = 30$ dBm.

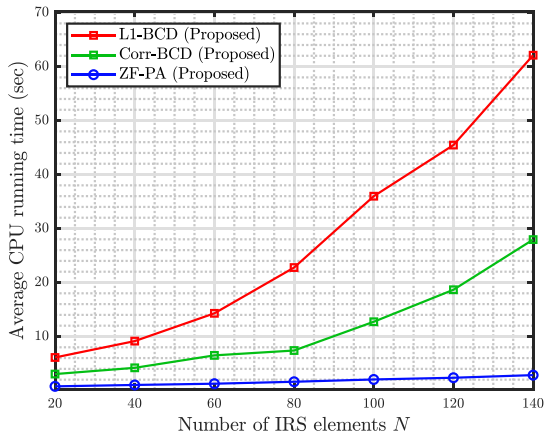


Fig. 4. Average CPU running time versus the number of IRS elements N for $M = 8, L = 3, K = 30, P = 30$ dBm.

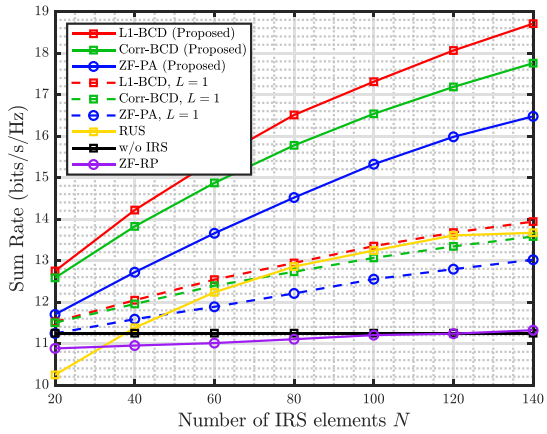


Fig. 5. Sum rate versus the number of IRS elements N for $M = 8, L = 3, K = 30, P = 30$ dBm.

by the proposed FP-based BCD algorithm described in Algorithm 3 without updating $\boldsymbol{\rho}$ and $\mathbf{u}$ in Step 7-8.

4) **ZF-based User Selection with Random phase (ZF-RP)**: In Algorithm 5, a random phase shift of IRS is used instead of adjusting it by (59).

In the following simulation results, we abbreviate the proposed l_1-norm based joint BS beamforming, IRS reflection coefficient design and user selection algorithm in Algorithm 3, correlation metric based user selection algorithm in Algorithm 4, and ZF beamforming based user selection algorithm in Algorithm 5 as **L1-BCD**, **Corr-BCD**, and **ZF-PA**, respectively.

B. Convergence and Complexity Analysis

Fig. 3 shows the convergence performance of our proposed algorithms. To verify the effectiveness of l_1-norm approximation based user selection, Fig. 3(a) presents the spectral efficiency of each user over the number of outer iteration I_3 in Algorithm 3 to maximize the sum rate. As shown in Fig. 3(a), the spectral efficiency of users who have less impact on maximizing the sum rate decreases over iterations and eventually becomes zero, resulting in their being unselected. The low power of the beamforming vector for those users can be reflected as a higher weight in (20) for each iteration, leading to their spectral efficiency decreasing to zero. On the other hand, the spectral efficiency of users who have a significant impact on maximizing the sum rate converges to a stable value and they are selected. This convergence result confirms that the l_1-norm approximation in (19) is effective in implicitly selecting users via optimizing the BS beamforming. The sum rate of selected users in our proposed algorithms are shown in Fig. 3(b). The sum rate performance of L1-BCD and Corr-BCD algorithms monotonically increases over iterations and converges to a local optimal solution within 30 iterations for different values of N, showing the robustness of the proposed algorithms. Also, the ZF-PA algorithm converges within 5 iterations for different values of N, showing the low complexity of this proposed algorithm.

Fig. 4 presents the average CPU running time of proposed algorithms with respect to the number of IRS elements. We can first observe that CPU running time is increasing with the number of IRS elements, which is confirmed in Table I. The L1-BCD algorithm requires the highest CPU running time since its complexity is of order $\mathcal{O}(N^3)$. Even though the Corr-BCD

Authorized licensed use limited to: Univ Of Incheon. Downloaded on October 26,2026 at 13:11:01 UTC from IEEE Xplore. Restrictions apply.

TABLE I
COMPUTATIONAL COMPLEXITY FOR PROPOSED ALGORITHMS

Algorithm	Computational Complexity
L1-BCD	$\mathcal{O}(I_3(I_1((MK)^3)+(LN)^3+I_2(LN)^2))$
Corr-BCD	$\mathcal{O}(KN^2M^2+I_3(I_1((M^2)^3)+(LN)^3+I_2(LN)^2))$
ZF-PA	$\mathcal{O}((M^2K+MN+M^2K^2)M)$

algorithm has the same complexity of $\mathcal{O}(N^3)$ as the L1-BCD algorithm, but Corr-BCD requires much fewer iterations for convergence and significantly lower CPU running time because it performs user selection in advance. In addition, as shown in Table I, the complexity of ZF-PA algorithm is of order $\mathcal{O}(N)$ which is the lowest complexity among proposed algorithms as confirmed in Fig. 4, because it simply aligns the IRS phase shifts to the nearest users.

C. Impacts of the Number of IRS Elements and IRSs

Fig. 5 presents the sum rate performance versus the number of IRS elements N. In this figure, we can observe that the sum rate of these algorithms are monotonically increasing with the number of IRS elements. Deploying the IRSs with the larger number of reflecting elements provides more capability for boosting received signal power and suppressing inter-user interference via reflected channel. Also, we can observe that the proposed algorithms achieve significant performance gain over benchmark schemes. Since the channel environment can be varied through IRS's reflected channel, the performance of user selection is affected by how the IRS phase shifts are controlled. Therefore, it is important to jointly select the appropriate users with the design of IRS phase shifts.

It can be observed that the performance of ZF-PA is worse than that of the other proposed algorithms. The ZF-PA algorithm aligns the phase shifts of each IRS with its nearest associated user to maximize the received channel gain for the specific user, without considering inter-user interference. Thus, this approach might result in a significant inter-user interference to other users near each IRS, while the other algorithms can reduce the inter-user interference by considering it when designing the IRS phase shifts. Nevertheless, the ZF-PA algorithm achieves almost 89% and 93% sum rate performance of L1-BCD and Corr-BCD, respectively, while achieving 5% and 10% average CPU time of L1-BCD and Corr-BCD, respectively, when $N = 120$. Additionally, this algorithm achieves 18% and 40% sum rate performance improvement compared to the RUS and w/o IRS benchmark schemes, respectively, when $N = 120$. Due to low complexity and satisfactory performance, the ZF-PA algorithm can be regarded as the candidate scheme for implementing it in a practical wireless network, especially when the number of IRSs and passive elements is large. In addition, a greedy user selection approach with ZF beamforming is widely used in practical systems such as 4 G LTE and 5 G NR [39], [40], and thus ZF-PA algorithm can be easily applied to future wireless network with multi-IRS.

Lastly, the L1-BCD algorithm provides the best performance, followed by the Corr-BCD algorithm and the ZF-PA algorithm. Therefore, it can be shown that there exists a trade-off between sum rate and complexity as shown in Figs. 4 and 5. Also, we confirmed that there is a similar tendency of sum rate performance with respect to the number of IRSs. It can be inferred that if more IRSs are deployed, the distance between IRSs and users may be shortened and the users are more likely to receive a better service from BS via reflected channels, and thus the sum rate would be monotonically increasing.

Fig. 6 illustrates the results of our proposed user selection algorithm (Algorithm 3) by comparing systems without IRS, IRSs with $N = 60$, and IRSs with $N = 240$. We choose $M = 4$, $K = 12$, $L = 3$ in this example. As shown in Fig. 6(a), when there are no IRSs, BS tends to select users having significant direct channel gains. However, when IRSs with the large number of elements are deployed as in Fig. 6(c), BS tends to select users near the IRSs, since these users can have more benefits of boosting received signal power and suppressing inter-user interference via reflecting channel. In the case of deploying IRSs with a modest number of elements as in Fig. 6(b), BS selects users having strong direct channel or strong reflected channel to strike a balance between them.

D. Impacts of the Number of Users

Fig. 7 presents the sum rate performance versus the number of users K and maximum selected users I. In our proposed algorithms, we assume that the number of maximum selected users is equal to the number of antennas. To show the effectiveness of I, we replace M into I in the constraint (15c) and Algorithm 3∼5 are slightly modified according to this replacement. First, in Fig. 7(a), we can observe that the sum rate of proposed algorithms is monotonically increasing with K, since it can exploit the multi-user diversity. It can be inferred from this figure that if more users are deployed, BS has a more opportunity to select users whose channels are close to pair-wise orthogonal while introducing a smaller inter-user interference. Then, BS can design beamforming vectors with lower power that guarantee the same performance as when the number of users is smaller and sum rate can be enhanced with the remaining power resources. Also, when comparing proposed algorithms to RUS algorithm, randomly selecting users not only cannot improve the performance even in the case with many users but also has a lower performance than system without IRS. Therefore, it is important to select appropriate users to enhance performance.

Second, in Fig. 7(b), we can observe that with the increase of I, the sum rate of all users first increases and then saturates. When I is small, the impact of the inter-user interference is not significant and it would be advantageous to choose more users having a better channel gain. However, when I is larger than a certain value, the impact of inter-user interference is dominant and selecting the all I users cannot guarantee the maximum sum rate. Moreover, when comparing L1-BCD algorithm to w/o IRS, we can observe that the saturation point is much larger in L1-BCD algorithm. This means that BS can support more users with the aid of IRSs, which validates the advantages of deploying multi-IRS and exploiting the multiple reflected signals.

It is interesting to note that the ZF-PA algorithm outperforms the Corr-BCD algorithm with small values of I. Since small

Authorized licensed use limited to: Univ Of Incheon. Downloaded on October 26,2026 at 13:11:01 UTC from IEEE Xplore. Restrictions apply.

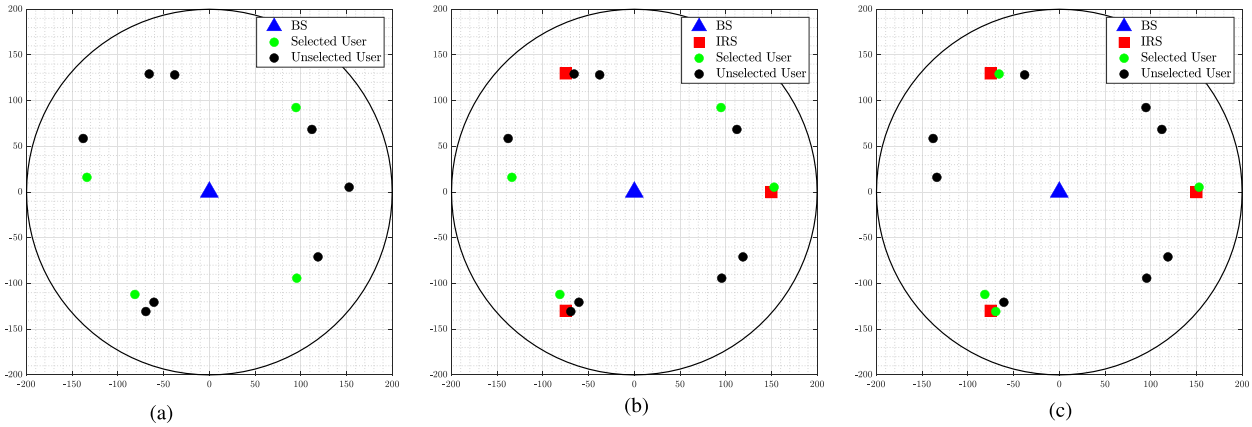


Fig. 6. Snapshot of user selection results obtained by Algorithm 3 for $M = 4, K = 12, L = 3$. (a) Without IRS. (b) IRS with $N = 60$. (c) IRS with $N = 240$.

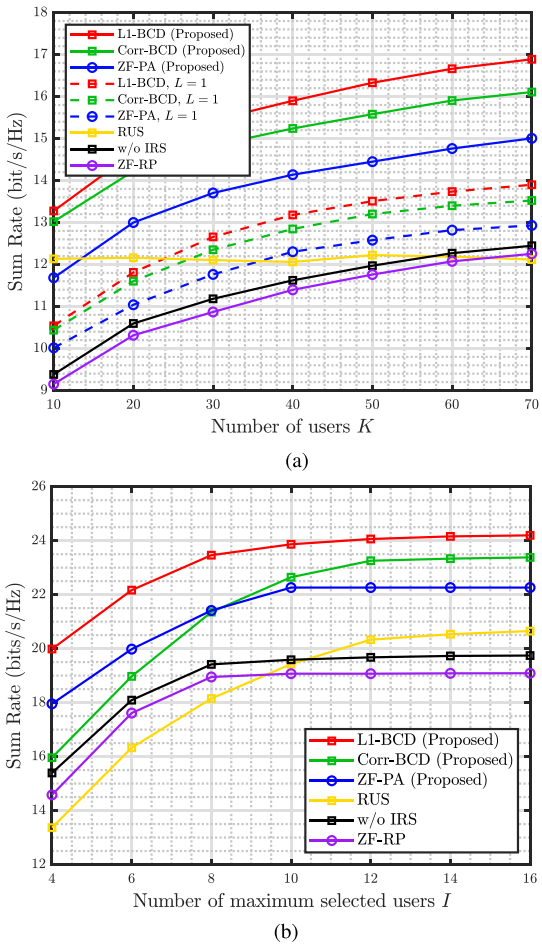


Fig. 7. Sum rate performance of proposed user selection algorithms in terms of users. (a) Sum rate versus the number of users K for $M = 8$. (b) Sum rate versus the number of maximum selected users I for $M = 16, L = 4, K = 40$.

values of I generate lower inter-user interference, boosting the channel gain by ignoring inter-user interference is advantageous for enhancing the sum rate compared to considering even a small amount of interference, which compromises the improvement of channel gain. As the number of selected users increases, the

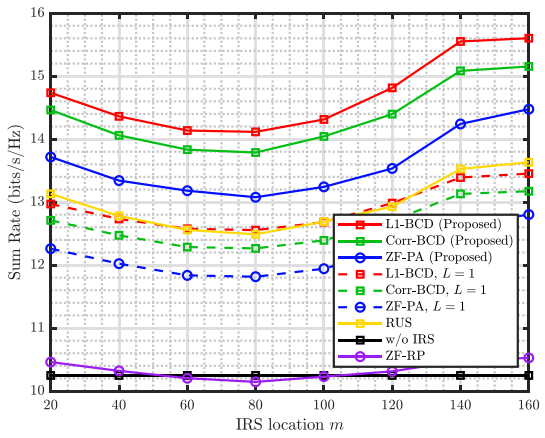


Fig. 8. Sum rate versus the IRS location for $M = 8, L = 3, N = 60, K = 30, P = 30$ dBm.

inter-user interference would be deteriorated, which should be considered for designing the IRS phase shifts and user selection. The ZF-PA algorithm cannot strike a balance between high inter-user interference suppression and channel gain improvement through phase alignment to a typical user and using ZF beamforming. The Corr-BCD algorithm, on the other hand, attains this balance by jointly optimizing the BS beamforming and IRS phase shifts, hence providing a better performance with large values of I. Lastly, it is observed that the L1-BCD algorithm, which jointly optimizes the BS beamforming, IRS phase shifts, and user selection while balancing signal power boosting and inter-user interference suppression, achieves the best balance and hence the best performance among the three algorithms.

E. Impacts of the IRSs Locations

Fig. 8 shows the sum rate performance versus the location of IRS where the distance between BS and user is set to 155m as an example. In this figure, we can observe that when the IRSs move away from BS towards the users, the sum rate first decreases and then increases. It can be inferred that double path

Authorized licensed use limited to: Univ Of Incheon. Downloaded on October 26,2026 at 13:11:01 UTC from IEEE Xplore. Restrictions apply.

losses of reflected channel in the case of deploying the IRSs near BS or users are much lower than the case of deploying the IRSs in the middle of BS and users. Also, the sum rate of deploying the IRSs near the users are slightly higher than the deploying IRSs near BS. This is because not only the Rician factor of BS-IRS channel is higher than the IRS-user channel but also it has the benefits of boosting the signal power and suppressing the interference when the users are close to IRSs. Moreover, our proposed algorithms always outperforms the other benchmark algorithms under different IRSs deployment settings.

IX. Conclusion

In this article, we proposed the joint optimization of BS beamforming, IRS reflection coefficients, and user selection to maximize the sum rate of selected users in a multi-IRS aided multi-IoT user system. After implicitly embedding the user selection variable in BS beamforming by using l_0-norm and weighted l_1-norm approximation, we developed an efficient FP-BCD algorithm which combines the Lagrangian sub-gradient method for the BS beamforming with the complex circle manifold (CCM) method for the IRS reflection coefficients to solve the non-convex problem. Furthermore, for reducing the computational complexity, we proposed two heuristic algorithms by employing a new correlation metric based user selection and a ZF beamforming based user selection. Numerical results validate the effectiveness and the performance gain of our proposed algorithms compared to benchmark algorithms under various system and network parameters.

Appendix A
Proof of Proposition 1

First, we define the $\tilde{f}_3(\boldsymbol{\eta}, \boldsymbol{\xi}, \mathbf{w}_k, \boldsymbol{\Theta}_l)$ and $\tilde{f}_4(\boldsymbol{\eta}, \mathbf{w}_k, \boldsymbol{\rho}, \boldsymbol{\Theta}_l)$ as follows

$$\tilde{f}_3(\boldsymbol{\eta}, \boldsymbol{\xi}, \mathbf{w}_k, \boldsymbol{\Theta}_l) = \sum_{k=1}^{K} w_k \log_2(1+\eta_k) - \sum_{k=1}^{K} w_k \eta_k + g_3(\boldsymbol{\eta}, \boldsymbol{\xi}, \mathbf{w}_k, \boldsymbol{\Theta}_l) \tag{63}$$

$$\tilde{f}_4(\boldsymbol{\eta}, \mathbf{w}_k, \boldsymbol{\rho}, \boldsymbol{\Theta}_l) = \sum_{k=1}^{K} w_k \log_2(1+\eta_k) - \sum_{k=1}^{K} w_k \eta_k + g_4(\boldsymbol{\eta}, \mathbf{w}_k, \boldsymbol{\rho}, \boldsymbol{\Theta}_l) \tag{64}$$

where g_3 and g_4 are the functions that include the remaining fixed variables in the functions f_{3b} and f_{4b}, respectively.

Then, we employ the following three lemmas for quadratic transform FP method in [30], which can be easily verified.

Lemma 1: $f_1(\mathbf{w}_k, \boldsymbol{\Theta}_l) \geq f_2(\boldsymbol{\eta}, \mathbf{w}_k, \boldsymbol{\Theta}_l)$ holds with equality if and only if $\boldsymbol{\eta}$ satisfies (24).

Lemma 2: $f_2(\boldsymbol{\eta}, \mathbf{w}_k, \boldsymbol{\Theta}_l) \geq \tilde{f}_3(\boldsymbol{\eta}, \boldsymbol{\xi}, \mathbf{w}_k, \boldsymbol{\Theta}_l)$ holds with equality if and only if $\boldsymbol{\xi}$ satisfies (27).

Lemma 3: $f_2(\boldsymbol{\eta}, \mathbf{w}_k, \boldsymbol{\Theta}_l) \geq \tilde{f}_4(\boldsymbol{\eta}, \mathbf{w}_k, \boldsymbol{\rho}, \boldsymbol{\Theta}_l)$ holds with equality if and only if $\boldsymbol{\rho}$ satisfies (42).

Using these lemmas, the non-decreasing of the objective function $f_1(\mathbf{w}_k, \boldsymbol{\Theta}_l)$ can be verified by considering the following series of inequalities.

$$\begin{aligned} f_1\left(\boldsymbol{\Theta}_l^t, \mathbf{w}_k^t\right) &\overset{(a)}{=} f_2(\boldsymbol{\eta}^t, \mathbf{w}_k^t, \boldsymbol{\Theta}_l^t) \\ &\overset{(b)}{=} \tilde{f}_3\left(\boldsymbol{\eta}^t, \boldsymbol{\xi}^{t+1}, \mathbf{w}_k^t, \boldsymbol{\Theta}_l^t\right) \\ &\overset{(c)}{\leq} \tilde{f}_3\left(\boldsymbol{\eta}^t, \boldsymbol{\xi}^{t+1}, \mathbf{w}_k^{t+1}, \boldsymbol{\Theta}_l^t\right) \\ &\overset{(d)}{\leq} f_2\left(\boldsymbol{\eta}^t, \mathbf{w}_k^{t+1}, \boldsymbol{\Theta}_l^t\right) \\ &\overset{(e)}{\leq} \tilde{f}_4\left(\boldsymbol{\eta}^t, \mathbf{w}_k^{t+1}, \boldsymbol{\rho}^{t+1}, \boldsymbol{\Theta}_l^t\right) \\ &\overset{(f)}{\leq} \tilde{f}_4\left(\boldsymbol{\eta}^t, \mathbf{w}_k^{t+1}, \boldsymbol{\rho}^{t+1}, \boldsymbol{\Theta}_l^{t+1}\right) \\ &\overset{(g)}{\leq} f_2\left(\boldsymbol{\eta}^t, \mathbf{w}_k^{t+1}, \boldsymbol{\Theta}_l^{t+1}\right) \\ &\overset{(h)}{\leq} f_2\left(\boldsymbol{\eta}^{t+1}, \mathbf{w}_k^{t+1}, \boldsymbol{\Theta}_l^{t+1}\right) \\ &\overset{(i)}{=} f_2\left(\mathbf{w}_k^{t+1}, \boldsymbol{\Theta}_l^{t+1}\right) \end{aligned}$$

where (a) follows from **Lemma 1**; (b) follows from **Lemma 2** and the step 5 of Algorithm 3; (c) holds because the update of $\mathbf{w}_k^{t+1}$ in step 6 of Algorithm 3 maximizes $\tilde{f}_3$ when the other variables are fixed; (d) follows from **Lemma 2**; (e) follows from **Lemma 3** and step 7 of Algorithm 3; (f) holds because the update of $\boldsymbol{\Theta}_l^{t+1}$ in step 8 of Algorithm 3 maximizes the $\tilde{f}_4$ when the other variables are fixed; (g) follows from **Lemma 2**; (h) holds because the update of $\boldsymbol{\eta}$ in step 9 of Algorithm 3 maximizes the $\tilde{f}_2$ when the other variables are fixed; (i) follows from **Lemma 1**. Therefore, we have proved that the objective function $f_1(\mathbf{w}_k, \boldsymbol{\Theta}_l)$ is non-decreasing over iterations.

References

[1] W. Saad, M. Bennis, and M. Chen, "A vision of 6G wireless systems: Applications, trends, technologies, and open research problems," *IEEE Netw.*, vol. 34, no. 3, pp. 134–142, May/Jun. 2020.

[2] Q. Wu, S. Zhang, B. Zheng, C. You, and R. Zhang, "Intelligent reflecting surface-aided wireless communications: A tutorial," *IEEE Trans. Commun.*, vol. 69, no. 5, pp. 3313–3351, May 2021.

[3] Q. Wu and R. Zhang, "Intelligent reflecting surface enhanced wireless network via joint active and passive beamforming," *IEEE Trans. Wireless Commun.*, vol. 18, no. 11, pp. 5394–5409, Nov. 2019.

[4] C. Huang, A. Zappone, G. C. Alexandropoulos, M. Debbah, and C. Yuen, "Reconfigurable intelligent surfaces for energy efficiency in wireless communication," *IEEE Trans. Wireless Commun.*, vol. 18, no. 8, pp. 4157–4170, Aug. 2019.

[5] H. Guo, Y.-C. Liang, J. Chen, and E. G. Larsson, "Weighted sum-rate maximization for reconfigurable intelligent surface aided wireless networks," *IEEE Trans. Wireless Commun.*, vol. 19, no. 5, pp. 3064–3076, May 2020.

[6] H. Xie, J. Xu, and Y.-F. Liu, "Max-min fairness in IRS-aided multi-cell MISO systems with joint transmit and reflective beamforming," *IEEE Trans. Wireless Commun.*, vol. 20, no. 2, pp. 1379–1393, Feb. 2021.

[7] G. Yu, X. Chen, C. Zhong, D. W. Kwan Ng, and Z. Zhang, "Design, analysis, and optimization of a large intelligent reflecting surface-aided B5G cellular Internet of Things," *IEEE Internet Things J.*, vol. 7, no. 9, pp. 8902–8916, Sep. 2020.

[8] J. Zuo, Y. Liu, Z. Qin, and N. Al-Dhahir, "Resource allocation in intelligent reflecting surface assisted NOMA systems," *IEEE Trans. Commun.*, vol. 68, no. 11, pp. 7170–7183, Nov. 2020.

[9] L. Wei, C. Huang, G. C. Alexandropoulos, C. Yuen, Z. Zhang, and M. Debbah, "Channel estimation for RIS-empowered multi-user MISO wireless communications," *IEEE Trans. Commun.*, vol. 69, no. 6, pp. 4144–4157, Jun. 2021.

Authorized licensed use limited to: Univ Of Incheon. Downloaded on October 26,2026 at 13:11:01 UTC from IEEE Xplore. Restrictions apply.

[10] Z. Wang, L. Liu, and S. Cui, "Channel estimation for intelligent reflecting surface assisted multiuser communications: Framework, algorithms, and analysis," *IEEE Trans. Wireless Commun.*, vol. 19, no. 10, pp. 6607–6620, Oct. 2020.
[11] L. Wei et al., "Joint channel estimation and signal recovery for RIS-empowered multiuser communications," *IEEE Trans. Commun.*, vol. 70, no. 7, pp. 4640–4655, Jul. 2022.
[12] X. Gan, C. Zhong, C. Huang, and Z. Zhang, "RIS-assisted multi-user MISO communications exploiting statistical CSI," *IEEE Trans. Commun.*, vol. 69, no. 10, pp. 6781–6792, Oct. 2021.
[13] Z. Li, M. Hua, Q. Wang, and Q. Song, "Weighted sum-rate maximization for multi-IRS aided cooperative transmission," *IEEE Wireless Commun. Lett.*, vol. 9, no. 10, pp. 1620–1624, Oct. 2020.
[14] P. Wang, J. Fang, X. Yuan, Z. Chen, and H. Li, "Intelligent reflecting surface-assisted millimeter wave communications: Joint active and passive precoding design," *IEEE Trans. Veh. Technol.*, vol. 69, no. 12, pp. 14960–14973, Dec. 2020.
[15] M. A. Saeidi, M. J. Emadi, H. Masoumi, M. R. Mili, D. W. K. Ng, and I. Krikidis, "Weighted sum-rate maximization for multi-IRS-assisted full-duplex systems with hardware impairments," *IEEE Trans. Cogn. Commun. Netw.*, vol. 7, no. 2, pp. 466–481, Jun. 2021.
[16] Z. Yang et al., "Energy-efficient wireless communications with distributed reconfigurable intelligent surfaces," *IEEE Trans. Wireless Commun.*, vol. 21, no. 1, pp. 665–679, Jan. 2022.
[17] H. Hashida, Y. Kawamoto, and N. Kato, "Selective reflection control: Distributed IRS-aided communication with partial channel state information," *IEEE Trans. Veh. Technol.*, vol. 71, no. 11, pp. 11949–11958, Nov. 2022.
[18] T. Yoo and A. Goldsmith, "On the optimality of multiantenna broadcast scheduling using zero-forcing beamforming," *IEEE J. Sel. Areas Commun.*, vol. 24, no. 3, pp. 528–541, Mar. 2006.
[19] G. Dimic and N. Sidiropoulos, "On downlink beamforming with greedy user selection: Performance analysis and a simple new algorithm," *IEEE Trans. Signal Process.*, vol. 53, no. 10, pp. 3857–3868, Oct. 2005.
[20] J. Choi, N. Lee, S.-N. Hong, and G. Caire, "Joint user selection, power allocation, and precoding design with imperfect CSIT for multi-cell MU-MIMO downlink systems," *IEEE Trans. Wireless Commun.*, vol. 19, no. 1, pp. 162–176, Jan. 2020.
[21] H. A. Ammar, R. Adve, S. Shahbazpanahi, G. Boudreau, and K.V. Srinivas, "Downlink resource allocation in multiuser cell-free MIMO networks with user-centric clustering," *IEEE Trans. Wireless Commun.*, vol. 21, no. 3, pp. 1482–1497, Mar. 2022.
[22] R. Huang and V. W. S. Wong, "Joint user scheduling, phase shift control, and beamforming optimization in intelligent reflecting surface-aided systems," *IEEE Trans. Wireless Commun.*, vol. 21, no. 9, pp. 7521–7535, Sep. 2022.
[23] A. Al-Hilo, M. Samir, M. Elhattab, C. Assi, and S. Sharafeddine, "Reconfigurable intelligent surface enabled vehicular communication: Joint user scheduling and passive beamforming," *IEEE Trans. Veh. Technol.*, vol. 71, no. 3, pp. 2333–2345, Mar. 2022.
[24] J. Kim, H. Lee, S.-E. Hong, and S.-H. Park, "A bipartite graph neural network approach for scalable beamforming optimization," *IEEE Trans. Wireless Commun.*, vol. 22, no. 1, pp. 333–347, Jan. 2023.
[25] S. Yang, W. Lyu, Y. Xiu, Z. Zhang, and C. Yuen, "Active 3D double-RIS-aided multi-user communications: Two-timescale-based separate channel estimation via Bayesian learning," *IEEE Trans. Commun.*, vol. 71, no. 6, pp. 3605–3620, Jun. 2023.
[26] V. Lau, "Proportional fair space-time scheduling for wireless communications," *IEEE Trans. Commun.*, vol. 53, no. 8, pp. 1353–1360, Aug. 2005.
[27] E. J. Candes, M. B. Wakin, and S. P. Boyd, "Enhancing sparsity by reweighted l_1 minimization," *J. Fourier Anal. Appl.*, vol. 14, no. 5, pp. 877–905, 2008.
[28] B. Dai and W. Yu, "Sparse beamforming and user-centric clustering for downlink cloud radio access network," *IEEE Access*, vol. 2, pp. 1326–1339, 2014.
[29] A. Ben-Tal and M. Zibulevsky, "Penalty/barrier multiplier methods for convex programming problems," *SIAM J. Optim*, vol. 7, no. 2, pp. 347–366, 1997.
[30] K. Shen and W. Yu, "Fractional programming for communication systems–Part II: Uplink scheduling via matching," *IEEE Trans. Signal Process.*, vol. 66, no. 10, pp. 2631–2644, May 2018.
[31] K. Shen and W. Yu, "Fractional programming for communication systems–Part I: Power control and beamforming," *IEEE Trans. Signal Process.*, vol. 66, no. 10, pp. 2616–2630, May 2018.
[32] M. Grant and S. Boyd, "CVX: Matlab software for disciplined convex programming, version 2.1," Mar. 2014. [Online]. Available: http://cvxr.com/cvx
[33] S. Boyd, L. Xiao, and A. Mutapcic, "Subgradient methods," lecture notes of EE392o, Stanford University, Stanford, CA, USA, 2003.
[34] G. Zhou, C. Pan, H. Ren, K. Wang, and A. Nallanathan, "A framework of robust transmission design for IRS-aided MISO communications with imperfect cascaded channels," *IEEE Trans. Signal Process.*, vol. 68, pp. 5092–5106, 2020.
[35] C. Pan et al., "An overview of signal processing techniques for RIS/IRS-aided wireless systems," *IEEE J. Sel. Topics Signal Process.*, vol. 16, no. 5, pp. 883–917, Aug. 2022.
[36] K. Alhujaili, V. Monga, and M. Rangaswamy, "Transmit MIMO radar beampattern design via optimization on the complex circle manifold," *IEEE Trans. Signal Process.*, vol. 67, no. 13, pp. 3561–3575, Jul. 2019.
[37] C. Pan et al., "Multicell MIMO communications relying on intelligent reflecting surfaces," *IEEE Trans. Wireless Commun.*, vol. 19, no. 8, pp. 5218–5233, Aug. 2020.
[38] K. Zhi, C. Pan, G. Zhou, H. Ren, M. Elkashlan, and R. Schober, "Is RIS-aided massive MIMO promising with ZF detectors and imperfect CSI?," *IEEE J. Sel. Areas Commun.*, vol. 40, no. 10, pp. 3010–3026, Oct. 2022.
[39] N. Prasad, S. Rangarajan, P. Wells, and R. Arnott, "Analysis and evaluation of a practical downlink multiuser MIMO scheduler over LTE advanced massive MIMO systems," U.S. Patent 10 334 616, Jun. 2019.
[40] C. Lim, T. Yoo, B. Clerckx, B. Lee, and B. Shim, "Recent trend of multiuser MIMO in LTE-advanced," *IEEE Commun. Mag.*, vol. 51, no. 3, pp. 127–135, Mar. 2013.



Seok-Hyun Yoon (Student Member, IEEE) received the B.S. degree in computer science and communication engineering from Korea University, Seoul, South Korea in 2017. He is working toward the Ph.D degree with the School of Electrical Engineering, Korea University. In 2022, he visited Tufts University, Medford, MA, USA, to conduct collaborative research. His research interests include mmWave/THz beamforming, intelligent reflecting surface, and full-duplex communication.



Byungju Lim (Member, IEEE) received the B.S. and Ph.D. degrees in electrical engineering from Korea University, Seoul, South Korea in 2015 and 2021, respectively. In 2021, he was a Research Professor with Korea University. From 2022 to 2023, he was a Postdoctoral Scholar with the Department of Electrical and Computer Engineering, Tufts University, Medford, MA, USA. Since 2023, he has been with the Department of Electronic Engineering, Pukyong National University, Busan, South Korea, where he is currently an Assistant Professor. His research interests include machine learning and signal processing for wireless communication.

Authorized licensed use limited to: Univ Of Incheon. Downloaded on October 26,2026 at 13:11:01 UTC from IEEE Xplore. Restrictions apply.



Mai Vu (Senior Member, IEEE) received the bachelor's degree in computer systems engineering from the Royal Melbourne Institute of Technology, Melbourne, VIC, Australia, M.S.E. degree in electrical engineering from the University of Melbourne, Parkville, VIC, and the Ph.D. degree in electrical engineering from Stanford University, Stanford, CA, USA. From 2006 to 2008, she was a Lecturer and a Researcher with the School of Engineering and Applied Sciences, Harvard University, Cambridge, MA, USA. From 2009 to 2012, she was an Assistant Professor of electrical and computer engineering with McGill University, Montreal, QC, Canada. Since 2013, she has been with Tufts University, Medford, MA, as an Associate then a Full Professor of electrical and computer engineering.

Dr. Vu conducts research in wireless systems, signal processing, and networked communications. She has published extensively in the areas of millimeter-wave communications, 5G and 6G systems, cooperative and cognitive communications, MIMO wireless, and energy-efficient communications. She was on the Technical Program Committee for numerous IEEE conferences. She was a Co-Organizer for the 2017 New England Workshop on Software Defined Radio (NEWSDR'17) at Tufts University and as a Technical Co-Chair of the 2023 IEEE Communication Theory Workshop (CTW), Taiwan. From 2013 to 2016, she was the Editor of the IEEE TRANSACTIONS ON WIRELESS COMMUNICATIONS. Since November 2022, she has been the Editor of the IEEE TRANSACTIONS ON COMMUNICATIONS.



Young-Chai Ko (Senior Member, IEEE) received the B.Sc. degree in electrical and telecommunication engineering from Hanyang University, Seoul, South Korea and M.S.E.E and the Ph.D. degrees in electrical engineering from the University of Minnesota, Minneapolis, MN, USA, in 1999 and 2001, respectively. In 2001, he was with Novatel Wireless as a Research Scientist. In 2001, he was with the Wireless Center, Texas Instruments, Inc., San Diego, CA, USA, as a Senior Engineer. He is currently a Professor with the School of Electrical Engineering, Korea University, Seoul. His research interests include performance analysis and the design of wireless communication systems.

Authorized licensed use limited to: Univ Of Incheon. Downloaded on October 26,2026 at 13:11:01 UTC from IEEE Xplore. Restrictions apply.